Journal of Industrial and Engineering Chemistry 151 (2025) 112–130

Contents lists available at ScienceDirect

Journal of Industrial and Engineering Chemistry

journal homepage: www.elsevier.com/locate/jiec

Review Article

Influence of Matrix, Filler, and structural design on the dielectric and energy storage properties of cellulose composites

Mohammed Arif Poothanari [a], Hanuma Reddy Tiyyagura [b], Yasir Beeran Pottathara [b,*]

[a] Department of Physics, MES College Nedumkandam, Chembalam, Idukki 685553 Kerala, India
[b] Rudolfovo-Science and Technology Center Novo Mesto, Podbreznik 15, 8000 Novo Mesto, Slovenia

A B S T R A C T

Cellulose is a renewable, biodegradable, cost-effective, and easy-to-process natural biopolymer. Because of its dielectric, piezoelectric, and mechanical performance, cellulose and its composites are often used as a matrix, filler, substrate, gel electrolyte, and dielectric layer for flexible energy storage devices. They offer easy fabrication strategies and excellent mechanical properties. In this mini-review, we summarized the principles of dielectric and energy storage features of cellulose composites and factors affecting their dielectric properties, mainly exploring the incorporation of various filler materials in the cellulose matrices and cellulose materials acting as different types of fillers. Moreover, the fabrication strategies, structural design, and matrix-filler interactions of cellulose composites enhance their dielectric properties as systematically reviewed. This review summarizes the current state-of-the-art progress of cellulose dielectric composites, challenges, and future outlook for green dielectric and energy storage devices. The review suggests that optimizing the filler type, cellulose fiber content, fabrication techniques, and structural design can significantly enhance the dielectric properties and energy storage capacity of cellulose composites.

Introduction

The pursuit of new materials with outstanding dielectric and energy storage properties has accelerated in recent years, driven by the ever-increasing demand for efficient energy storage systems and high-performance electronic devices. It is high time to develop new green energy sources and storage technologies as the energy consumption pattern abruptly upsurges. The non-biodegradable and non-renewable synthetic polymer-based composites can cause severe contamination to nature due to the frequent replacement rate of electronic devices. Thus, it is having great significance to develop new biodegradable and renewable high performing dielectric and energy storage materials for flexible electronics. In this scenario, cellulose composites have garnered significant attention due to their unique combination of environmental friendliness, mechanical robustness, and versatile functionalization capabilities [1]. Moreover, the energy storage competence of dielectric materials is a critical factor in the performance of capacitors, which are essential components in numerous electronic devices, power systems, and emerging technologies like electric vehicles and renewable energy grids. Traditional dielectric materials, often derived from petrochemical sources, pose significant environmental concerns and limitations in their performance. In contrast, cellulose composites offer a sustainable alternative, potentially bridging the gap between high performance and eco-friendliness.

Cellulose, a naturally abundant and renewable biopolymer, is an ideal material for developing biodegradable dielectric and energy-storing materials due to its high surface area, excellent mechanical strength, and tunable porosity. The large number of hydroxyl groups on the molecular chain provides additional dipole moments. So, cellulose offers a biodegradable and eco-friendly alternative to synthetic polymers, aligning with the trend around the world towards eco-friendly and sustainable materials [2,3]. Its inherent properties, such as high mechanical strength, biodegradability, and ease of chemical modification, make it an exceptional base material for composite fabrication [4–6]. However, pristine cellulose is not an ideal dielectric material to achieve the required performance of energy storage material, and its hydrophilic nature could decrease the energy storage density. Nonetheless, its ability to be engineered at the molecular level to enhance the dielectric constant and breakdown strength of composites is promising. Therefore, cellulose-based composites with outstanding performance for dielectric and energy storage devices have become a research hotspot.

Integrating cellulose with advanced fabrication techniques can

Abbreviations: BC, Bacterial Cellulose; CA, Cellulose Acetate; CEC, Cyanoethyl Cellulose; RC, Regenerated Cellulose; MC, Methyl Cellulose; CMC, Carboxymethylcellulose; CNF-, Cellulose nanofibrils; CNC, Cellulose nanocrystals; ATO, Antimony tin oxide; $BaTiO_3$, Barium titanate; TiO_2, Titanium dioxide; MAA, Methacrylic acid; MMPR, Methacrylate malate photocurable resin; PANI, Polyaniline; PDMS, Polydimethylsiloxane; PDA, Polydopamine; PVDF, Polyvinylidene fluoride; PC, poly (bisphenol A carbonate); PVA, Polyvinylalcohol.

* Corresponding author.
E-mail address: yasir.beeran@rudolfovo.eu (Y.B. Pottathara).

https://doi.org/10.1016/j.jiec.2025.04.025
Received 15 December 2024; Received in revised form 17 March 2025; Accepted 10 April 2025
Available online 16 April 2025

revolutionize the field of dielectric materials, aligning with the global imperative for sustainable development[7,8]. The fabrication strategy of cellulose composites is a critical determinant of the microstructure and, consequently, the macroscopic properties of cellulose composites. For instance, solution casting/filtration/drying [9] can lead to uniform films with controlled thickness, while electrospinning [10] can produce nanofibrous mats with high surface area. Layer-by-layer assembly [11] allows for precise control over the composite architecture, in-situ polymerization [12], and 3D printing [13] opens new avenues for creating complex geometries tailored to specific applications. A variety of hydrophobic modification techniques have been devised to prevent water absorption in high-humidity conditions and enhance the energy storage density of cellulose composites. The main methods to improve hydrophobicity include surface deposition [14], graft modification [15], and polymer interpenetrating networks [16]. Each method offers distinct advantages and challenges, influencing filler dispersion, interfacial interactions, and mechanical properties.

It is evident from Fig. 1 that there has been a substantial rise in the number of publications on cellulose composites for dielectric and energy storage in recent years. This increase indicates that these composites, which combine cellulose with nanomaterials/ polymers, have become a significant area of research for developing sustainable materials for energy applications. By providing a comprehensive overview of the current state and future prospects, this review aims to serve as a valuable resource for researchers and engineers striving to develop next-generation energy storage solutions. Moreover, it provides a detailed examination of the state-of-the-art cellulose composite, focusing on how different fabrication strategies impact their dielectric and energy storage properties. To our knowledge, the effect of structural designs and various fabrication strategies on the dielectric and energy storage properties of cellulose composites and the overview of recent progress have not been summarized in the last decade.

The key objectives of this review are the following. (i) To elucidate the fundamental dielectric properties of cellulose and its derivatives: Understanding the intrinsic properties of cellulose is crucial for tailoring its performance in composite materials. (ii) To assess the role of matrices and fillers: The incorporation of ceramics, metal oxides, and nanomaterials, such as graphene, carbon nanotubes, and metallic nanoparticles, in cellulose matrix as well as cellulose as filler material, can significantly enhance the dielectric and energy storage properties of cellulose composites. (iii) To analyze various fabrication techniques, structural design, and their influence on composite performance: The fabrication strategy plays a pivotal role in determining the final properties of cellulose composites. (iv) To identify future research directions: Highlighting gaps in current knowledge and proposing potential pathways for future investigations to advance the field of cellulose-based dielectric materials to elucidate the fundamental dielectric properties of cellulose and its derivatives.

Principles of dielectric and energy storage properties

Theory of dielectric

Dielectrics are materials that an electric field can polarize. They can also have an electrostatic field within them. High-quality thin films possessing high strength, low loss, and high dielectric constant are essential for dielectric polymer capacitors to be designed compactly. Dielectric materials can show high dielectric constant and dielectric loss under alternating electric fields because of their slower interfacial polarization response [17]. This phenomenon can occur in a dielectric material or a capacitor component, typically at frequencies below 100 Hz. Dielectric responses in polymers are usually related to three types of polarization: dipolar, atomic, and electronic polarization [18,19]. Dielectric material polarization processes as a function of frequency, as seen in Fig. 2.

Dipolar polarization is the relaxation of dipoles in response to an alternating field. Dipolar polarization occurs in a broad frequency of up to 10^8 Hz and exhibits high dielectric constants. Upon removing the applied field, quick relaxation of dipoles results in a shorter relaxation time. Atomic polarization is caused by nucleus displacement responding to electric fields up to 10^{13} Hz. Electron polarization happens when electrons move under an electric field until the ultraviolet frequency (10^{15} Hz) [20,21]. When the frequency of an electric field becomes very high, the dipoles present in the material may not be able to keep up with the rapid changes in the direction of the applied field. Then, a phase difference arises between the dipoles' orientation and the field's

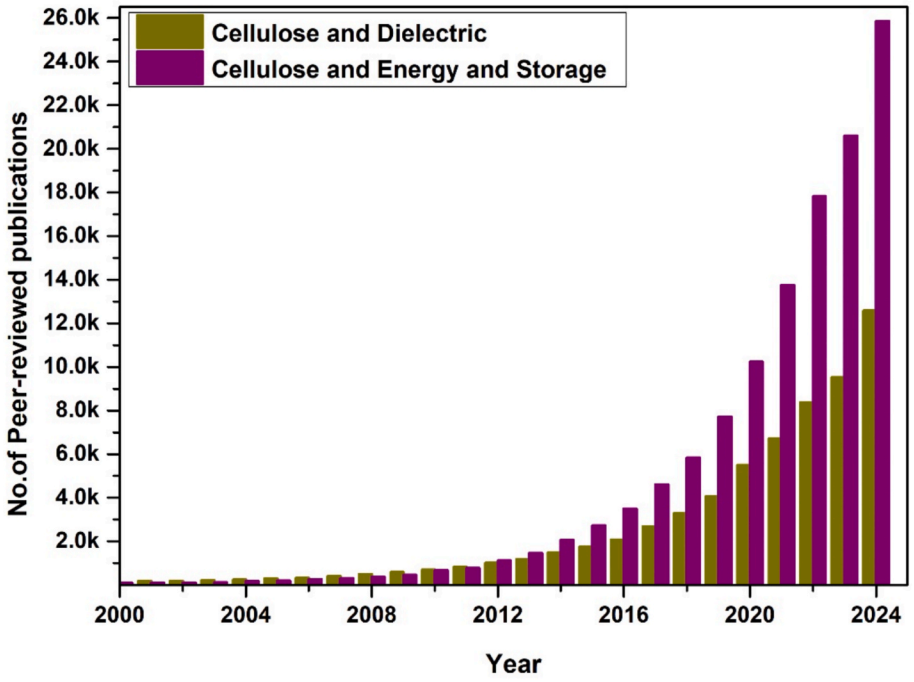

Fig. 1. Peer-reviewed publication statistics on cellulose composites for dielectric and energy storage from January 1, 2000, to December 10, 2024, data from Scopus.

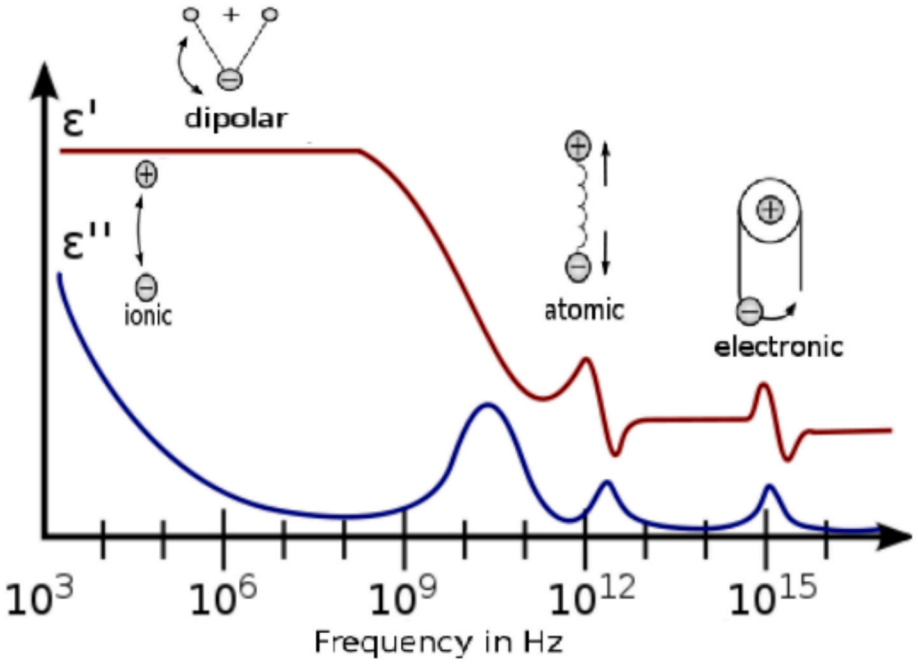

Fig. 2. Dielectric constant and Dielectric loss of dielectric materials against frequency [20].

direction [22]. When exposed to high-frequency alternating electric fields, the dielectric response of materials is influenced by the amplitude and frequency of the field, the temperature, and the material's molecular structure [23]. The quantity of water in materials and agricultural goods modifies their dielectric characteristics. Another element influencing the dielectric characteristics of particulate materials is the bulk density of the air-particle combination. The chemical composition of a material, which includes mobile ions and dipole moments from compounds like water, determines its dielectric characteristics [24].

Under a high-frequency alternating electric field, permanent dipoles lag with the applied field, producing a phase difference (δ) between the electric field and electric displacement [25].

$$D_0\exp[i(wt-\delta)\,] = \varepsilon^*\varepsilon_0 E_0\exp[i(wt-\delta)\,]$$

where E_0 and D_0 are the amplitudes of the applied field and electric displacement, and ε* is the dielectric permittivity determined as:

$$\varepsilon^* = \varepsilon' - \varepsilon''$$

where ε' is the real and ε'' the imaginary part of permittivity; ε'' is also meant to be a dielectric loss. The ε' and ε'' are calculated using the following equations [26].

$$\varepsilon' = C_p d/\varepsilon_0 A$$

$$\varepsilon'' = \varepsilon' \tan\delta$$

$$\sigma_{ac} = 2\pi f \varepsilon_0 \varepsilon''$$

where ε_0 is the permittivity of free space, C_p is parallel capacitance, d is the thickness of the sample, A is the area of the sample, tanδ is the tangent loss, σ_{ac} is the AC conductivity, and f is the frequency. The real component indicates the dielectric material's capacity to store energy in the electric field, while the imaginary part denotes the dielectric's capacity to dissipate energy, which allows energy from the electric field to be transformed into heat energy within the dielectric [27,28]. Piezoelectrics, ferroelectrics, and pyroelectrics are some dielectric materials that may exhibit polarization without an external electric field [25,29].

Polymers are materials that consist of flexible chains with dipoles attached to them. When exposed to a field, the dipoles can align themselves more easily with the applied field if the chain is more flexible. Additionally, the crystallinity phase can also affect the orientation of dipoles. Crystalline regions can restrict the capacity of dipoles to be oriented with the field [30,31]. The dielectric properties of polymers are complex because they contain a mixture of permanent and induced dipoles of various sizes and masses. This complexity is further influenced by the interactions that occur between the dipoles and their surrounding molecules. Polymer nanocomposites are heterogeneous compositions consisting of two or more components, such as polymers and fillers. Interfacial polarization (Maxwell_Wagner_Sillars effect) is present in polymer composites, particularly in the case of a conductive filler, in polymer matrix [32,33]. The significant rise of the interfacial area in polymer nanocomposites establishes interfacial polarization as the dominant physical factor influencing their electrical and dielectric properties. Different theoretical approaches have been discussed in the literature on the permittivity of nanocomposites. The Lichtenecker logarithmic rule gives the effective permittivity of two-component composites based on the volume-fraction average. Lichtenecker's logarithmic equation is given [34]:

$$log\varepsilon = \phi_1 log\varepsilon_1 + \phi_2 log\varepsilon_2$$

where ϕ1 and ϕ2 represent the volume fractions of fillers and polymer matrix, and ε1 and ε2 denote permittivity values of filler and polymer, respectively. The Bruggeman model provides the effective permittivity of the two-phase composite [35]:

$$\phi_1\left(\frac{\varepsilon_1 - \varepsilon}{\varepsilon_1 - 2\varepsilon}\right) + \phi_2\left(\frac{\varepsilon_2 - \varepsilon}{\varepsilon_2 - 2\varepsilon}\right) = 0$$

The Bruggeman model is based on a mean-field approximation of spherical inclusions enclosed by a polymer matrix. The Bruggeman model suggests that for volume fractions higher than 20 %, the dielectric constant of nanocomposites increases sharply. The effective-medium theory (EMT) involves averaging the dielectric permittivity of two phases and fitting parameters to address the shape of the filler [36].

Theory of energy storage

Energy storage systems, including electrical, magnetic, mechanical, chemical, and thermal, can be used in various ways. Electrostatic and magnetic systems store energy in an electric field, with capacitors and supercapacitors classified as electrostatic systems and superconducting magnetic energy storage (SMES) as a magnetic system.[37]. Dielectrics are ideal for storing electrical energy due to their polarization ability and capacity increase. Capacitors store energy through an electrostatic field with metal plates separated by a dielectric layer. The energy density of a linear dielectric is determined using a specific relation [25]:

$$U = \frac{1}{2}\varepsilon_0 \varepsilon' E^2$$

where E is the electric field's intensity, ε' is the dielectric constant, and $\varepsilon_0 is$ permittivity of free space.

In this context, the electric field serves as a representation of the operational parameters of the capacitive system and is independent of the chosen dielectric material. The only physical characteristic included in the equation is the real component of the dielectric permittivity. Therefore, given identical operating circumstances, the material with the most efficient energy storage capacity has the greatest dielectric permittivity. The electric field value determines the highest amount of stored energy, after which dielectric breakdown takes place, and the dielectric material collapses. It is necessary to choose materials that possess both high dielectric constant and high dielectric breakdown strength for a high energy density storage system. The determination of the stored and harvested energy may be achieved by considering both the charging and discharging processes in the capacitive system. Estimation of stored energy may be derived using the following equation [25]:

$$Storedenergy = \frac{1}{2}\frac{Q^2}{C}$$

where Q is the accrued charge, and C is the capacitance.

Inorganic materials can have a high dielectric permittivity but low breakdown strength. Polymers have a high breakdown strength and low energy density due to their low dielectric permittivity. In polymer nanocomposites, combining polymers with high breakdown strength and inorganic materials with excellent permittivity gives substantial energy storage capacity.

The probability of failure/breakdown of nanocomposites can be estimated using the Weibull function [38,39].

$$P(E) = 1 - exp\left(-\frac{E}{E_b}\right)^{\beta}$$

where E is the experimental breakdown strength, E_b is the Weibull breakdown strength with a 63.2 % probability of breaking down, and β is a shape parameter. Wu et al. used the Weibull function to study the breakdown strength of PVDF-graft copolymer/cyanoethyl cellulose (CEC) composites [40]. They plotted electric field strength versus $ln[-ln(1-P(E))]$ of the PVDF-graft copolymer/CEC composites, as shown in Fig. 3. The breakdown strength of the composites gradually decreased as CEC increased.

Characteristics of a nanocomposite are determined by its components and the interactions taking place at the interface of the system. Nanoparticles, such as ceramic nanoparticles, carbides, or carbon nanoforms, can add high dielectric properties to composite systems. If the nanoparticles are finely dispersed, they create a network-like structure of nanocapacitors that are capable of being charged and released at specified requests, allowing for energy storage and harvesting at the nanoscale. The effective energy density of composites can be represented by an equation [35]:

$$U_e = \phi_1 U_e^{(1)} + \phi_2 U_e^{(2)} + gU^{(3)}$$

where ϕ_1 and ϕ_2 represent the volume proportion of the component materials, $U_e^{(1)}$ and $U_e^{(2)}$ represent the energy densities of the component materials , g is proportional to the energy density contribution from the interfacial region, and $U^{(3)}$ is the energy density associated with the contact between the constituent materials. For the nanocomposite to show a significant energy density, it is crucial to have high energy

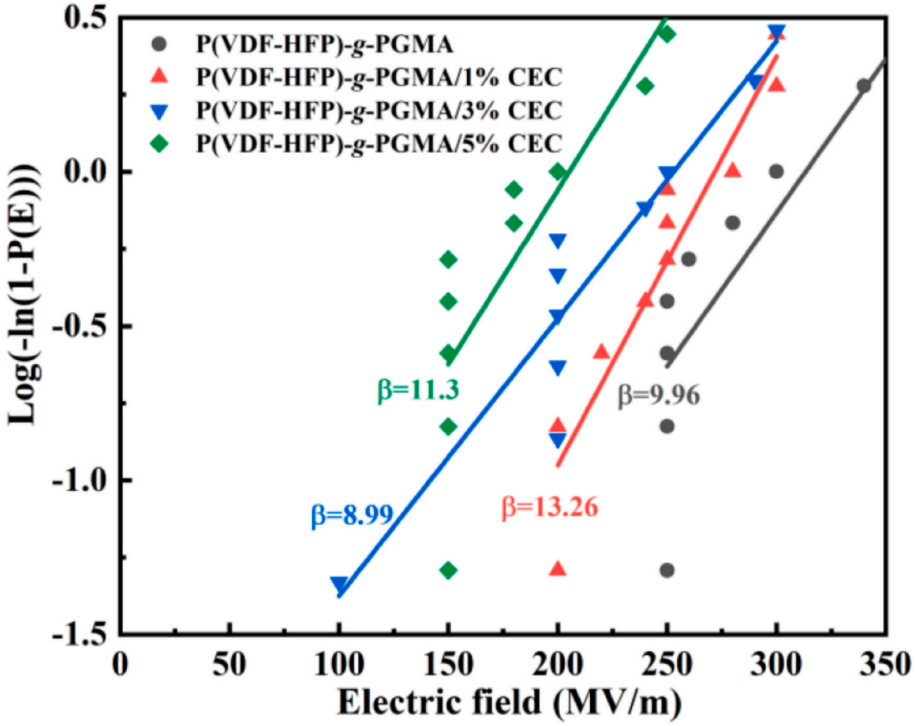

Fig. 3. Weibull distribution of the breakdown strength of the PVDF-graft copolymer/CEC composites [40].

densities from both phases and good dispersion of fillers in the matrix. Modifying the interface of polymer chains-nanofiller will enhance stored and recovered energy capacity [41]. This opens new possibilities for developing lightweight, efficient, and movable gadgets that deal with energy at the nanoscale level. Synthetic polymer-based materials used in electronics are problematic due to their non-biodegradable and non-renewable nature, which causes severe contamination. There is a growing need for decomposable and sustainable high-dielectric materials. Cellulose, with its unique properties, is a promising option for biodegradable dielectric materials[42]. It has exceptional mechanical properties and is decomposable and biocompatible. However, cellulose's hydrophilicity can decrease energy-storing capacity in a high-humidity environment[16]. Researchers focus on developing cellulose composites for capacitors that offer excellent overall performance.

Dielectric and energy storage performance of cellulose composites

Cellulose composites as renewable dielectric materials are of hot research topic as they electrostatically store energy via dielectric polarization for numerous applications in flexible electronics. Such energy storage technologies require excellent characteristics such as high charge–discharge efficiency, high power density, and long-term stability to be applied in electric vehicles and power systems [43]. Many researchers paid their attention to exploring the dielectric and energy storage performance of pristine cellulose and its composites fabricated via various processing techniques. The recent progress of dielectric and energy storage properties of cellulose-based composites has been detailed in Tables 1 and 2, respectively.

Transparent regenerated cellulose (RC) dielectric films have been reported via simple dissolution of cellulose in H_2SO_4 aqueous solution and showed excellent discharged energy density of 16.78 J/cm^3 at a breakdown strength of 500 MV/m[44]. The planar orientation of the hydroxyl group of cellulose and the film surface appears to be parallel, and this results in a stronger hydrogen bonding and leads to high dielectric constant and high polarization. The study found that cellulose-based dielectric films should be stored in a dry environment or treated for hydrophobic modification to enhance their dielectric performance. The breakdown strength of the cellulose films shows enhancement with respect to the film density. Cotton cellulose and PVDF were co-dissolved as a matrix film, and $BaTiO_3$ nanoparticles were incorporated to offer high energy storage performance, as reported by Zhang et al.[45]. The strong hydrogen bonding between PVDF and cellulose molecules enhances polarization intensity, the film exhibits an energy storage density of 8.29 J/cm^3 for 3.20 MV/cm. Upon incorporating the $BaTiO_3$ nanoparticles, the resultant film shows a remarkable breakdown strength of 3.70 MV/cm and an energy storage density of 10.81 J/cm^3. As from Fig. 4, the cellulose80/PVDF20 (C8/P2) film showed excellent performance with the highest maximum polarization (P_m) and remnant polarization (P_r) near the electrical breakdown strength (E_B) among all other pristine organic films. This would be accredited to the strong hydrogen bonds by hydroxyl groups, contributed from cellulose, and fluorine atoms, contributed from PVDF, which provide more dipoles and, thereby, the highest polarization. Transparent dielectric films with TEMPO-oxidized cellulose nanofibril (CNF) and PVDF nanoparticles were fabricated via solution-casting technique by Goodman *et* al. and achieved a high energy density of 7.22 Jcm^{-3} at a breakdown strength of 388 MVm^{-1}[46]. This composite offers a power density of ~3 MWcm^{-3} under an applied field of 300 MWm^{-1} over 1000 charge/discharge cycles.

Table 1
Dielectric properties of cellulose-based composites.

Cellulose composites	Dielectric constant	Dielectric loss	Ac conductivity (S/m)	Tan δ	Frequency	Reference
CNC/graphene oxide	652	1.8	–	–	1 kHz	[47]
CEC/TiO_2	207	–	–	< 0.3	1 kHz	[48]
CEC/ $BaTiO_3$	27.24	0.3	–	–	1 kHz	[49]
RC/CNT	1580	12	–	–	100 Hz	[50]
CA/ Al_2O_3 nanosheets	27.57	0.64	–	–	50 Hz	[51]
CEC/reduced graphene oxide	125	0.7	–	–	1 kHz	[52]
CNF/N-graphene oxide	46	–	2.07×10^{-4}	–	1 MHz	[53]
TEMPO CNF/ N-graphene oxide	52	–	3.46×10^{-4}			
CNF/reduced graphene oxide	164	–	0.0072	–	1 MHz	[54]
CNF/PANI/PVA	8x10^7	15	3-		100 Hz	[55]
CNF/CNT	3198	~ 1			1 kHz	[56]
MCC/PMMA	~ 6.5	–	1.4×10^{-4}		1 kHz	[57]
CNF/ graphene oxide (GO)	88.9	–	9.37×10^{-4}		1 MHz	[58]
MC/nicotinic acid	13.88	–	–	–	1 MHz	[59]
RC/ Al_2O_3 nanosheets	10.1	0.016	–	–	1 kHz	[60]
RC/$BaTiO_3$ nanoparticles	12	0.02	–	–	100 Hz	[61]
RC/$BaTiO_3$ nanofibers	13.3	0.02				
CNF/ $BaTiO_3$	188.03	–	–	1.21	1 kHz	[9]
TEMPO CNF/ graphene oxide (GO)	119.2	–	0.0053	–	1 MHz	[62]
CNF/multi-walled carbon nanotubes (MWCNT)	73.88	–	1.77×10^{-5}	0.68	1 kHz	[63]
Cyanoethyl cellulose/ $BaTiO_3$	44	0.01	–	–	1 kHz	[64]
CNC-MAA/MMPR	10.9	0.787	–	–	1 kHz	[65]
Cellulose powder/PDMS	7.3	0.07	–	–	1 kHz	[66]
Cellulose powder/Au nanoparticle/PDMS	7.7	0.04				
Cellulose with epichlorohydrin (ECH)	9.7	0.01	–	–	1 kHz	[67]
Cellulose/PDMS	6.25	0.06	–	–	1 kHz	[68]
BC/skim natural rubber latex	170	76	–	–	100 Hz	[69]
CNF/TiO_2	19.51	0.81	–	–	1 kHz	[70]
TEMPO CNF/ TiO_2	47.15	3.32				
CMC/PVDF-Epoxy- $BaTiO_3$ nanoparticles	292	0.1	–	–	1 kHz	[71]
CEC/ ATO-$BaTiO_3$	147.3	~4.3	3.11×10^{-6}		100 Hz	[72]
MCC/MXene	11.63	5.6	–	0.4	2 GHz	[73]
CNF/PANI/PVA	38	–	~ 13	~ 0.7	8.5 GHz	[74]
CNF/PANI	1.66	0.47	–	–	10 GHz	[75]
CEC/rGO/MMT	728	–	–	–	20 Hz	[76]

Table 2
Energy storage properties of cellulose-based composites.

Cellulose composites	Energy storage density (J/cm^3)	Breakdown strength (MV/m)	Charge-discharge efficiency	Energy storage density after 10,000 cycles (J/cm^3)	Reference
RC/PVDF	8.3	410	–	–	[16]
RC/ Al_2O_3 nanosheets	6.2	420	93 %	1.7 @200MV/m	[60]
RC/ Al_2O_3 nanosheets/PVDF	8.3	400	>80 %	2.1 @200MV/m	[60]
RC/ flyash (FA) coated PDA	3.47	330	–	–	[77]
TEMPO CNF/PVDF	7.22	388	–	–	[46]
CNF/CNT	0.81 ± 0.1	0.425	–	–	[56]
TEMPO CNF-Eu	1.5	208	–	–	[78]
TEMPO CNF-Na	0.08	52			
RC/$BaTiO_3$ nanoparticles	9.43	390	–	–	[61]
RC/BaTiO3 nanofibers	13.14	370			
RC/$BaTiO_3$ nanofibers/PDA	–	–	91 %	3.1 @200MV/m 6.4 @300MV/m	[79]
RC/ Al_2O_3 nanoparticles	5.7	380	–	–	[80]
Cellulose with epichlorohydrin (ECH)	2.16	–	>85 %	–	[67]
RC/$NaNbO_3$ nanowires	12.1	450	>80.1 %	–	[81]
CEC/Boron nitride nanosheets	23.5	680	83.6 %	–	[82]
Cellulose/ boron nitride nanosheet	4.1	370	–	–	[83]
CNF/boron nitride nanosheet	3.90	370	83 %	–	[84]

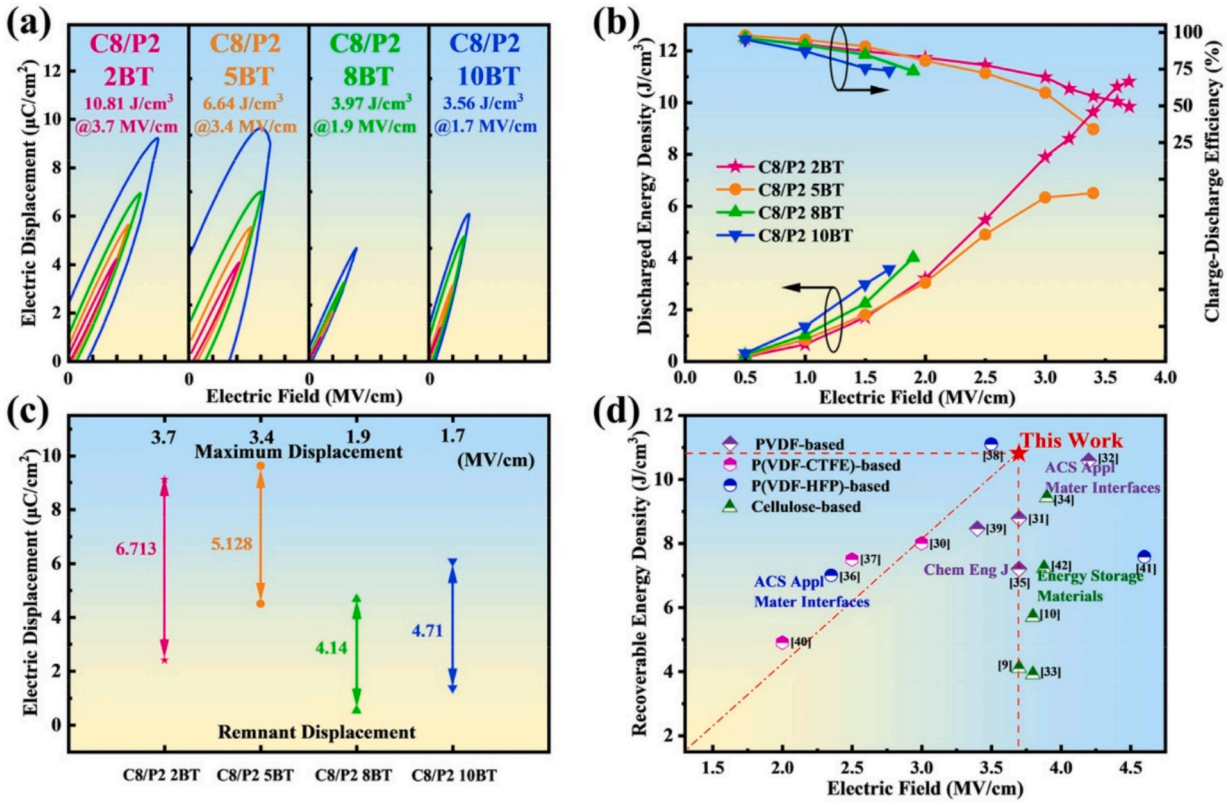

Fig. 4. (a) Polarization-electric field (P-E) loops of Cellulose/PVDF- $BaTiO_3$ (BT) films at 100 Hz; (b) discharged energy density and efficiency of films at different electric fields; (c) Pm-Pr values of films; (d) comparisons of the maximum recoverable energy densities and the corresponding electric field strength of PVDF-based, P(VDF-CTFE)-based, P(VDF-HFP)-based and cellulose-based composites. Reprinted with permission from Elsevier [45].

Influence of Composites: Cellulose as matrix materials

Ceramic fillers

The cellulose film is limited in application in certain fields due to its low toughness and poor optical, dielectric, and electrical performance [50]. To overcome these limitations, ceramic nanofillers like barium titanate ($BaTiO_3$) and titanium dioxide (TiO_2) can be incorporated into the polymer matrix to create high-performance nanocomposites. Barium titanate has an excellent dielectric constant (~7000) [9], a low loss factor, and notable piezoelectric and pyroelectric properties [85]. Therefore, incorporating ceramics nanoparticles into polymers is an efficient technique for developing high-performance nanocomposites with high dielectric permittivity [86,87]. To give an example, adding

strontium, $BaTiO_3$ nanorods, modified $BaTiO_3$ nanorods, and calcium copper titanate ($CaCu_3Ti_4O_{12}$) nanorods to the poly(arylene ether nitrile) (PEN) matrix made the composites excellent at the dielectric values and energy density values[88–90].

Tao et al. created composite films of $BaTiO_3$ and CNF, achieving a dielectric value 7 times higher than pure CNF without significantly altering the loss factor [50]. Zhang et al. fabricated PVDF-epoxy blend nanocomposites with carboxymethyl cellulose-$BaTiO_3$ (BT-CMC) network structure for energy storage applications [71]. The nanocomposite showed a high dielectric constant of 292 and a low loss factor of less than 0.1 at 31 vol% of $BaTiO_3$. The energy density of the nanocomposites with 25 vol% of $BaTiO_3$ is 15.7 $\times$ 10^{-3} Jcm^{-3} at 100 kV/cm, which is 3.48 times higher than the polymer matrix. Jia et al. fabricated cyanoethyl cellulose/$BaTiO_3$ nanocomposite films [49]. CEC has excellent heat and acid resistivity, low moisture regains, and suitable mechanical properties. CEC with a high substitution degree demonstrates a high dielectric constant and relatively low loss factor. It provides excellent water, insulation resistance, and self-extinguishing properties, and it possesses antimicrobial properties [72,91]. It found that incorporating $BaTiO_3$ nanofillers in the CEC matrix improved the dielectric constant of CEC while having less effect on the loss factor of the films. The composite films show a high dielectric constant of 27.24 at 1 k Hz with $BaTiO_3$ at 90 %, and the dielectric loss was 0.3023. In another work, using the solution blending method, the same group developed CEC nanocomposite films of $BaTiO_3$ and antimony tin oxide (ATO) as fillers [72]. They found that the dielectric loss of CEC/$BaTiO_3$/ATO film decreased after the addition of $BaTiO_3$, which is ascribed to better dispersion of ATO and prevents the creation of conductive paths of ATO and leakage current will be blocked successfully. The dielectric permittivity of CEC/$BaTiO_3$/ATO nanocomposite was as high as 147.30 at 100 Hz with 30 wt% of $BaTiO_3$ and 28 wt% of ATO. The CEC/TiO_2 nanoparticles nanocomposite films exhibited high dielectric constants of 118, 176, and 207 at 1 kHz for 10 %, 20 %, and 30 %wt. of TiO_2, respectively [48]. Wang et al. fabricated CEC/boron nitride nanosheets decorated $BaTiO_3$ nanoparticles-based nanocomposite films[64]. The fabricated composite films show a dielectric constant of 44, a breakdown strength of 302 kV/mm, and a low loss factor of 0.01. Lao et al. produced nanocomposite films of regenerated cellulose and boron nitride nanosheet (BNNS) with good energy density and electrical breakdown strength [83]. The research found that the cellulose molecules stabilize boron nitride nanosheets and enhance the dielectric constant films. It was observed that adding 10 wt% of BNNS in the nanocomposite film gives an energy storage density of 4.1 J cm^{-3} and a breakdown voltage of 370 MVm^{-1}. Zhang et al. developed regenerated cellulose/$BaTiO_3$ films by the addition of $BaTiO_3$ nanoparticle (BTNP) or nanofiber (BTNF) [61]. A composite film containing 2 % BTNF exhibited a discharged energy density of 13.14 J/cm^3 at 370 MV/m. At 300 MV/m, the RC-2BTNF exhibited the greatest discharged energy density among dielectric films made of polymers, with a value of 9.45 J/cm^3. Fig. 5 shows a Weibull curve indicating the breakdown strength of RC, RC-BTNP, and RC-BTNF composite films. It shows that breakdown strength increases with BTNP and BTNF concentration. Yin et al. developed flexible regenerated cellulose/dopamine-modified $BaTiO_3$ nanofiber nanocomposite films [79]. The cellulose nanocomposite films containing 2 vol% PDA-BTNF exhibited a discharged energy density of 17.1 J/cm^3 at 520 MV/m. The RC-2PDA/BTNF films operate continuously beyond 10,000 cycles with a high efficiency of 91 %. Menazea et al. developed PEO/CMC/MoO_3 nanobelts blend nanocomposites[92]. The addition of MoO_3 nanobelts to the PEO/CMC matrix significantly increases the dielectric constant and loss due to enhanced parallel dipolar ordering of C–O–C, C—O, and –OH groups. This suggests potential use in various optoelectronic devices. The research also shows that ceramic fillers enhance dielectric characteristics and energy storage capabilities.

Conductive fillers

Ceramic/polymer composites often require a larger amount of filler to achieve good dielectric properties [93]. However, this can cause severe agglomeration, poor mechanical strength, and low breakdown

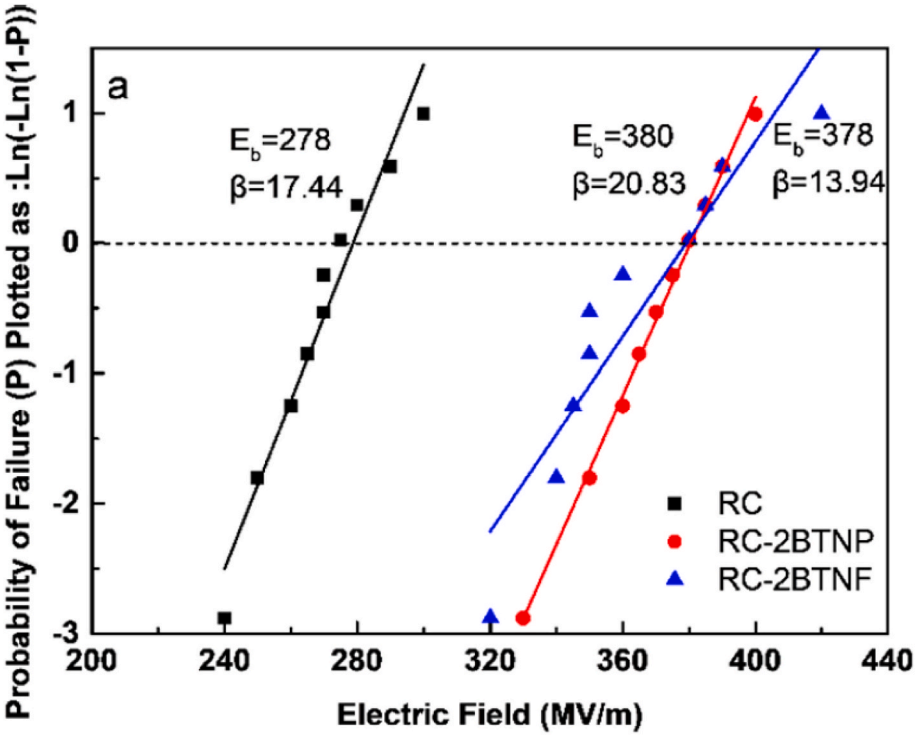

Fig. 5. The Weibull plot of the breakdown strength of RC, RC-2BTNP, and RC-2BTNF.
Reproduced with permission from the American Chemical Society 61.

resistance. On the other hand, adding a small amount of conductive filler can remarkably increase the dielectric constant and other physical properties. As stated by percolation theory, the dielectric properties increase rapidly around the threshold filler loading, typically below 5 % for raw fillers and even lower for treated fillers [94]. Different types of conductive fillers, such as carbon nanotubes, graphene, carbon nanofibers, silver nanowires, and polyaniline (PANI), are used for cellulose-based composites in dielectric and energy applications.

Raghunathan et al. fabricated regenerated cellulose/carboxyl-modified carbon nanotube (f-CNT) films, and dielectric studies showed that dielectric permittivity increases with f-CNT addition [50]. The composite with f-CNT1 % film displays a dielectric constant of 1580 and a low loss factor of 12 at 100 Hz; the films could be suitable for capacitor applications. Zeng et al. fabricated CNF/CNT flexible papers by vacuum-assisted self-assembly method, and the fabricated paper shows a permittivity of 3198 @1 kHz and energy storing capacity of 0.81 J cm^{-3} at 4.5 wt% CNTs loading [56]. Fig. 6 shows that the energy density of CNF/CNT thin films increases with CNT loading, attributed to the enhancement of dielectric properties after 4 wt% CNT loading. The breakdown strength reduced with CNT loading, and the paper showed (@4.5 wt% CNT) a breakdown strength of 425.8 kV cm^{-1}, which is ideal for energy storage applications.

Tao et al. reported that acid oxidization of MWCNTs improved the dielectric value from 25.24 for CNF to 73.88 for CNF/MWCNT thin film. In contrast, the dielectric loss and AC conductivity were decreased. The addition of MWCNTs enhanced the thermal and mechanical performance of the developed films [95]. Gopakumar et al. investigated the microwave absorbing, dielectric, and electrical performance of CNF/polyaniline papers [75]. They found the shielding effectiveness of the nanopapers was ~ 23 dB for 1.0 mm paper at 8.2 GHz. The nanopaper shows the dielectric value of 1.66 for 10 GHz and 1.26 for 15 GHz. In another work, Anju et al. investigated the EMI shielding performance of PVA-PANI and carbon nanofiber or nitrocellulose (NFC) hybrid composite films [74]. They achieved shielding effectiveness of 31.5 dB in the S-band region and –33.6 dB in the X-band range for 0.11 mm films. The PANI/carbon nanofiber /PVA films show a dielectric value of 62 at 8.55 GHz, whereas the PANI/NFC/PVA films show a lower value. They also studied the dielectric properties of PANI-coated cellulose fiber/PVA composite films [96]. Three sizes of cellulose fibers were utilized: macro, micro, and nano. The composites fabricated using nanocellulose fibers display high dielectric properties. This outcome showcases how the nanostructural filler can impact the macroscopic properties of the composites by changing the interfacial polarization. Beeran et al. have developed cellulose films by adding ammonia-functionalized graphene oxide (NGO) to the CNF and 2,2,6,6-tetramethylpiperidin-1-yloxyl TEMPO-oxidized (TCNF) CNF matrices [97]. The incorporation of NGOs has led to remarkable improvements in the dielectric properties of the fabricated films. At 1 MHz, the dielectric value of the CNF/3 wt% NGO and TCNF/3 wt% NGO films has enhanced significantly from 7.5 and 9.7 to 46 and 51.5, respectively, with respect to the neat CNF and TCNF films. To evaluate the composite films' energy storage capability and electrochemical performance, cyclic voltammetry and electrochemical impedance investigations have been conducted. The same research team utilized UV treatment under nitrogen gas atmosphere to develop reduced graphene oxide (GO) in CNF films [98]. After 5 hrs of UV treatment, a film loaded with 3 wt% graphene oxide enhanced its dielectric constant from 68.9 to 88.9. Fig. 7 illustrates the dielectric value and ac conductivity of CNF films added with GO, both with and without UV irradiation**.** The same group conducted another study that looked at the dielectric performance of UV treatment in the nitrogen atmosphere to create films of reduced graphene oxide (GO) and TEMPO-oxidized cellulose nanofibers [99]. The study found that the composite film of TCN/3 wt% NGO, treated for 5 h with UV, had a dielectric constant of 119.2 at a high frequency of 1 MHz. The results show that compared to solvent-based approaches, UV light in the presence of CNF to reduce GO is a potential option.

In a graphene oxide-based hybrid cyanoethyl cellulose composite film, $BaTiO_3$ was incorporated as the second filler, and it showed a higher dielectric value of 1505 at 100 Hz compared to the cyanoethyl cellulose/$BaTiO_3$ composite [100]. Wang et al. fabricated a composite film consisting of cyanoethyl cellulose, reduced graphene oxide (rGO), and montmorillonite (MMT) clay. The rGO acted as a conductive filler,

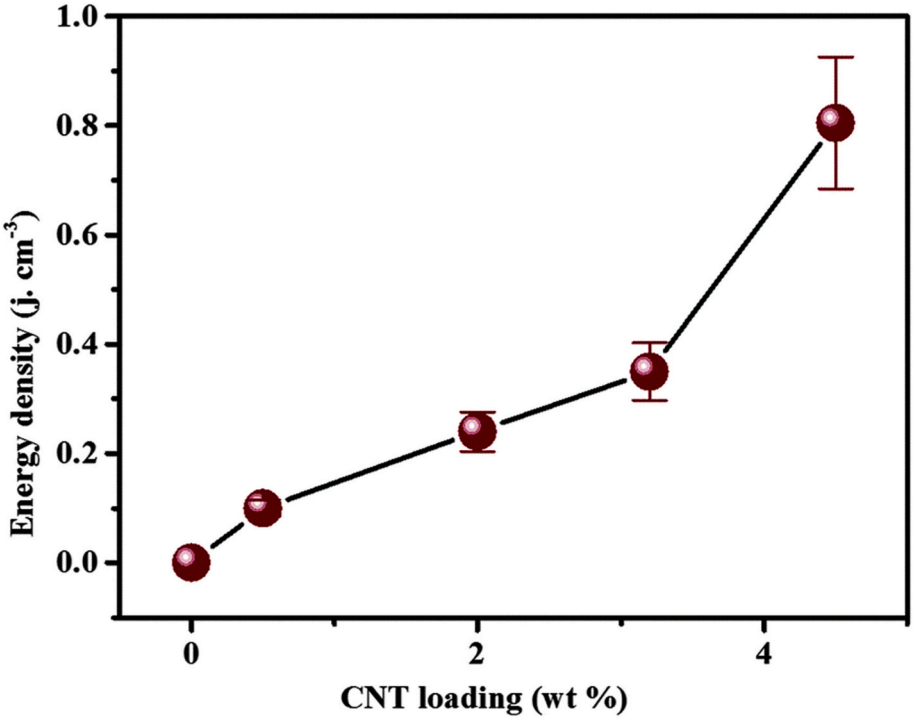

Fig. 6. The energy density of the CNF/CNT paper films versus CNT loadings. Reproduced with permission from the Royal Society of Chemistry 56.

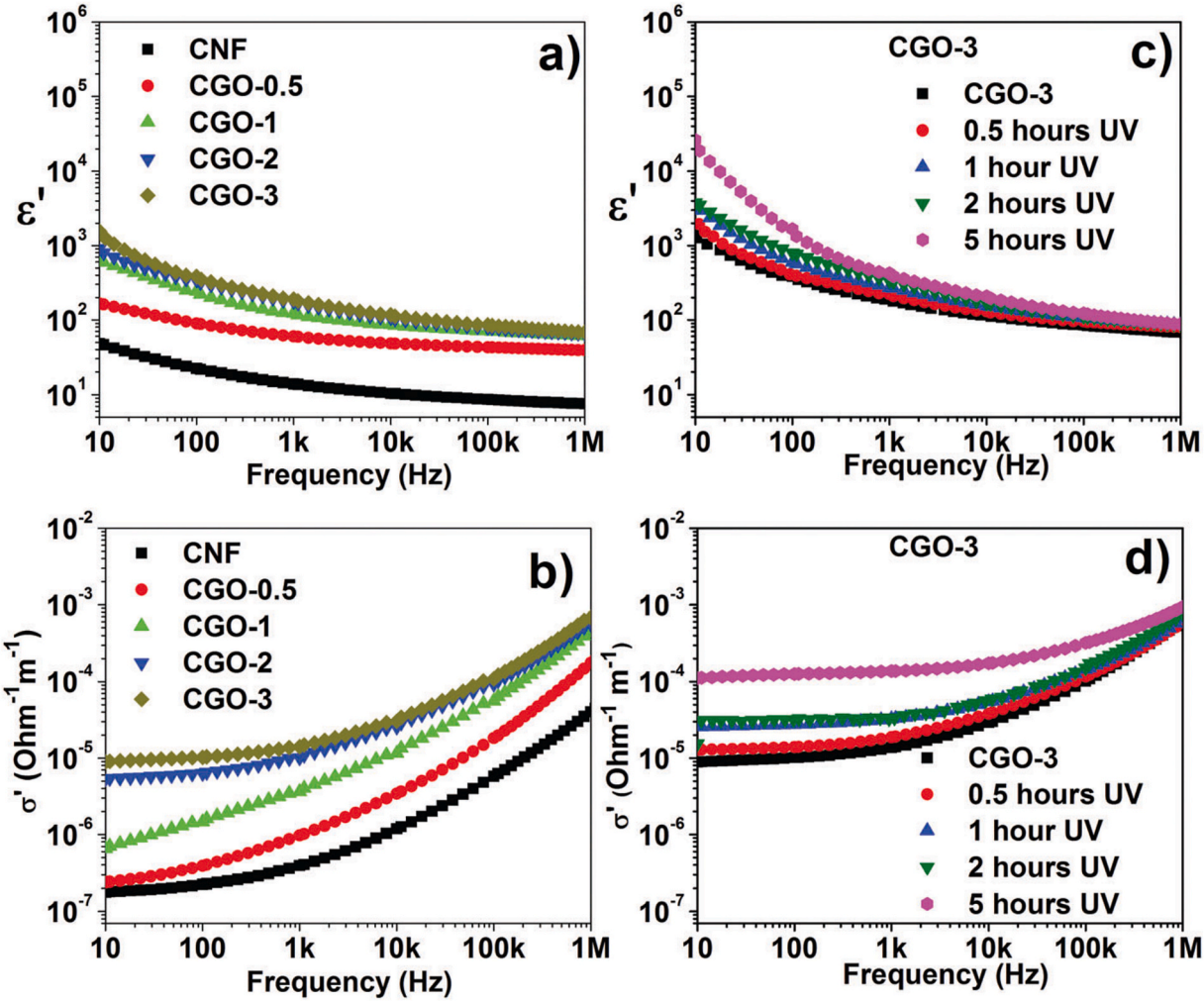

Fig. 7. (a) Frequency versus dielectric constant ε′ and (b) AC conductivity σ′ for CNF loaded with 0.5, 1, 2, and 3 wt% GO. (c) Frequency versus dielectric constant ε′ and (d) AC conductivity σ′ for CGO-3 treated for 0.5, 1, 2, and 5 hrs by UV.
Reproduced with permission from the Royal Society of Chemistry 58.

while the MMT served as a disperser of graphene [101]. When 6.8 % rGO and 3.4 % MMT were incorporated, the resulting CEC/rGO/MMT composite had a high dielectric value of 125 and a low loss of 0.7 at 1 kHz.

Metal oxides

Incorporating inorganic ceramic and conductive fillers into a matrix is an easy and useful way to enhance the energy storage properties of polymer composites. Nevertheless, the dielectric constant of these fillers differs significantly from that of the polymer matrix, leading to an uneven distribution of the internal electrical field in composite materials. This can lead to the materials breaking down at relatively low field strength [60]. To address this issue, metal oxide nanofillers are commonly used to create innovative polymer nanocomposites for optoelectronics and organic electronic devices. Furthermore, the high thermal conductivity of metal oxide nanoparticles allows them to efficiently dissipate the thermal energy within the matrix when a field is applied. This helps to reduce the chance of a thermal breakdown of the material [102].

Laila et al. developed thin films of Polyethylene oxide (PEO), CMC (Carboxymethyl cellulose), and ZnO/GO nanoparticles as nanofillers [103]. The incorporation of ZnO/GO has improved the optical, dielectric, and electrical properties of the PEO/CMC composite films. They reported that by elevating the amount of ZnO/GO NPs, the nanocomposites' dielectric properties were improved significantly. Yang et al. fabricated luminescent cellulose nanofibril (oxidized with 2,2,6,6-tetramethyl-piperidine-1-oxyl radical) films (TOCN) with europium/sodium carboxylate groups [78]. The films provide enhanced mechanical characterizations, resistance to water, thermal stability, oxygen-barrier characteristics, breakdown strength, and energy density. The TOCN-Eu film exhibited a breakdown strength of 208 MV m^{-1}, which is a fourfold value compared to the breakdown strength of the TOCN-Na film (52 MV m^{-1}). The presence of robust ionic interactions between the carboxylate groups and the Eu^{3+} ions is the cause of this phenomenon. The discharged energy density of the TOCN-Eu1 film was 1.50 J cm^{-3} at 200 MV m^{-1}, much more than the discharged energy density of the TOCN-Na1 film (0.08 J cm^{-3} at 50 MV m^{-1}). Zheng et al. reported the energy density of regenerated cellulose/Al_2O_3 nanosheet film of 5 wt % Al_2O_3 nanosheets filler shows 6.2 J/cm^3 @420 MV/m, which is twofold higher than that of regenerated cellulose [60]. They also developed an interpenetrating network structure of RC/PVDF/Al_2O_3 nanosheet composite film with a high energy density. RC/5 wt% Al_2O_3 nanosheets/3 wt% PVDF shows of energy density of 8.32 J/cm^3 at 400 MV/m and functions consistently at 200 MV/m for 10,000 cycles. The composite films showed significantly improved dielectric properties at high humidity compared to RC. Adding Al_2O_3 nanosheets and PVDF materials into the regenerated cellulose matrix caused no disruption to

the stability of the cycle and provided excellent dispersion inside the cellulose matrix, whereas PVDF generally displayed prominent distribution at the periphery. Fig. 8 displays the dielectric properties, discharge energy density, and charge–discharge efficiency of RC/PVDF/Al_2O_3 composite films. Sriphan et al. developed a bacterial cellulose (BC)/titanoniobate (Ti_2NbO_7) nanosheet-based triboelectric nanogenerator [76]. The fabricated cellulose composite film shows a dielectric of 728 at 20 Hz for 30 vol% Ti_2NbO_7. The good dielectric values of the cellulose composites improved the efficiency of the fabricated triboelectric nanogenerator. Dielectric and energy storage properties of cellulose composites are summarized in Table 1.

Influence of Composites: Cellulose as a filler material

Cellulose fillers offer many advantages, such as biodegradability and abundance, compared to synthetic fillers. The addition of such fillers in polymer composites affects their dielectric behavior. Different forms of cellulose, such as CNF, cellulose nanocrystals (CNC), BC, etc., are often used as filler materials in polymer composites to improve the overall performance of dielectric and energy storage properties as they complete the deficits of composites' properties. The type, amount, and particle size/aspect ratio of cellulose filler and adhesion between them impact the thermomechanical and dielectric properties of resultant composites. High aspect ratio fillers generally offer high dielectric properties, even at lower filler volume fractions [104]. The amount of hydroxyl groups present in the cellulose filler would influence compatibility with the polymer matrix, resulting in variations in the strength of the composites. However, cellulose possesses some drawbacks, such as poor dimensional stability and low heat resistance.

The amount of cellulose as a filler material is an important factor in influencing the dielectric properties of composites. Polyaniline (PANI) coated cellulose fibers have been fabricated as filler material in polyvinyl alcohol composites with superior dielectric permittivity and minimal percolation threshold [105]. As shown in Fig. 9, the reported dielectric constant for short cellulose composites is 2.3 x 10^5 at 40 Hz, and for micro and nanocellulose fiber composites is 4.5 x 10^5 and 1.3 x 10^8. The higher amount of cellulose exhibits a percolation threshold of 20 % at a frequency of 1 kHz. The composite shows a dielectric loss of 101, and the ac conductivity is 3 S/m, which is attributed to forming a percolating network of PANI-coated cellulose fibers in the polyvinyl alcohol matrix. The dielectric constant shows an increment with the increased mass fraction of PANI-coated cellulose filler due to the incorporation of polar groups in the PVA matrix. At a higher aspect ratio of fillers, their interaction will be higher, which results in the formation of effective networks. Moreover, the Maxwell-Wagner-Sillars (MWS) effect, charge accumulation at the interfaces between matrix and filler, will occur as the aligned cellulose fibers at the interface create an active conductive network [106]. Fig. 9 shows the variations in dielectric constants with macro, micro, and nano-sized cellulose composites. The maximum filler content, 80 %, offers the highest dielectric constant at all frequency ranges. It is worth noting that a minimum filler content is required to form a percolative network in cellulose composites, and beyond this point, a micro-capacitor or nano-capacitor formation is the reason for higher dielectric performance.

Composites of natural rubber with cellulose fillers (CNF and CNC) as a filler material have been reported with increased dielectric loss with the increase of cellulose fillers [107,108]. Here, the larger amount of cellulose mass fraction upsurges the water absorption capacity, leading to the monomolecular layer formation on the filler surface. In cellulose composites, two dielectric relaxation peaks are reported at low temperatures, where the hydroxyl connection between water and matrix composites may be caused, and at high temperatures, where the charge mobility will increase, thereby increment of dielectric constant and dielectric loss properties. Ladhar *et* al. reported various relaxation phenomena, such as lignin and hemicellulose relaxation, α dipole relaxation, water dipole relaxation, and ionic conduction [109]. Cellulose is often considered a hybrid filler, along with other biopolymer fillers, to improve the solubility in matrices and develop dielectric

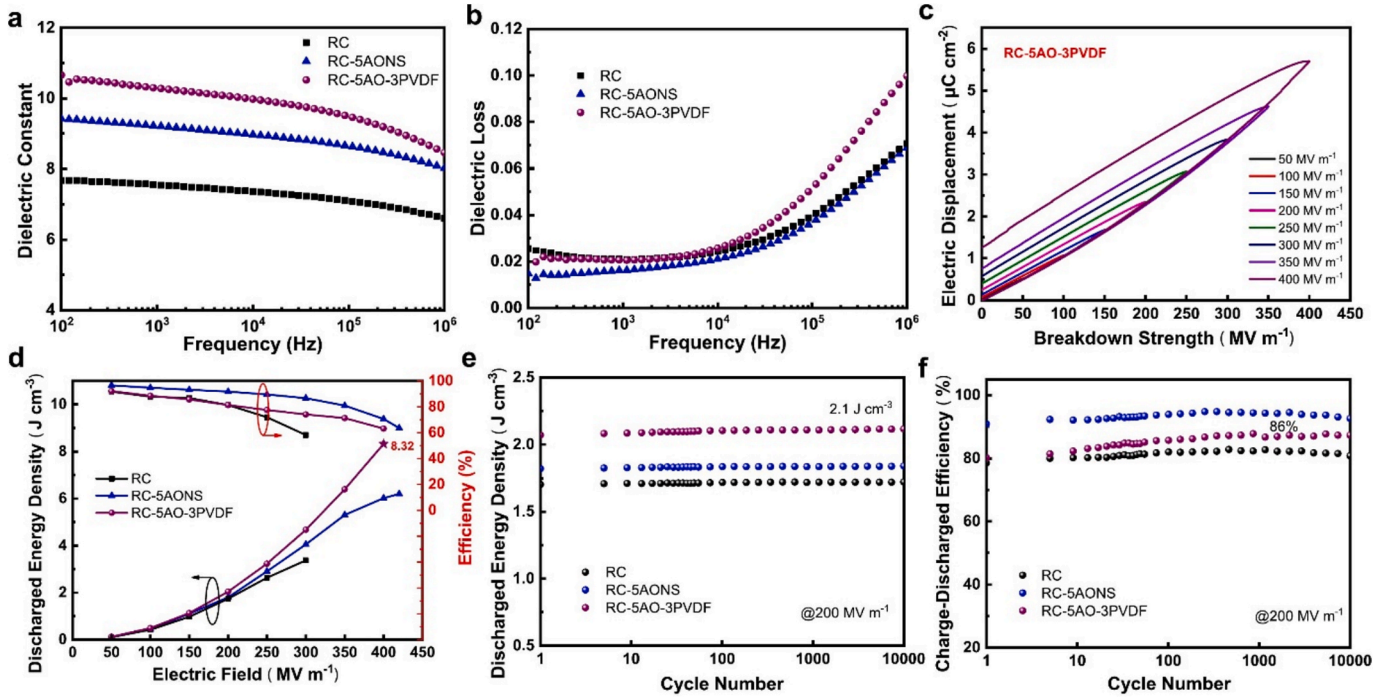

Fig. 8. Frequency versus (a) the dielectric constant and (b) the loss factor of regenerated cellulose (RC), RC- 5 wt% Al_2O_3 nanosheets (5AONS) and RC- 5 wt% Al_2O_3 nanosheets- 3 wt% PVDF (RC-5AO-3PVDF) (c) D-E loops of the RC-5AO-3PVDF composite film; (d) discharged energy density and charge–discharge efficiency of RC, RC-5AONS and RC-5AO-3PVDF (e) discharged energy density and (f) charge–discharge efficiency of RC, RC-5AONS and RC-5AO-3PVDF composites cycle for 10,000 times at 200 MV/m.
Reproduced with permission from Elsevier 60.

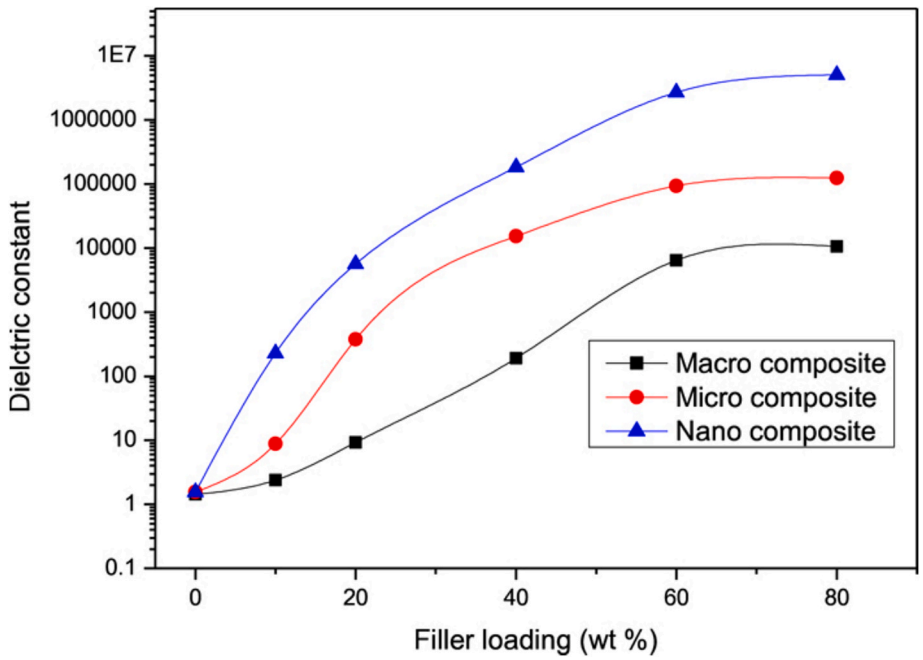

Fig. 9. Dielectric constants of PANI-coated cellulose/PVA composites at a frequency of 1 kHz. Reprinted with permission from AIP Publishing [105].

composites. A cellulose-based hybrid filler was reported by chybczyńska *et* al. to offer high mechanical, magnetic, and dielectric properties [110]. Incorporating the hybrid filler into the chitosan matrix hinders the molecular motions of all relaxation processes and lowers the activation energy. A cellulose–fiber framework has been incorporated into the PVDF and PC (PVDF-PC) matrix and showed an increased dielectric permittivity and dielectric loss of about ~81 and 10^{-2}, respectively [111]. The enhanced dielectric performance has been explained in three aspects: dipole polarization, interfacial polarization, and surface effect. The cellulose-fiber framework offers insulating properties to the composite and fills the interspaces between PVDF and PC microspheres, which leads to the blocking of carrier migration of the conduction path and thereby somewhat declines the dielectric loss.

Recently, cellulose fibers incorporated plasticized cellulose acetate biocomposites have been reported with enhanced dielectric properties [112]. Adding 50 wt% of cellulose fibers provided an ε' value of about 4 and a tan δ value of 0.13 at a frequency of 1 MHz. At a frequency of 3 GHz, the dielectric properties showed a decreased value of 2.8 and 0.04 for ε' tan δ. They also studied the dielectric performance with temperature variations and noted an increased dielectric constant at 80 °C. The addition of cellulose fibers introduces polar groups into the polymer matrix, which leads to dipolar polarization, thus improving the dielectric constant and the loss factor. Such a trend has already been reported, and increased fiber content consequently increases the composite's density and, thereby, the dielectric performance [113]. Fig. 10 shows that the dielectric properties show a linear increase corresponding to fiber content. Improved dielectric constant with a higher cellulose filler content has been reported with the same group for cellulose fibers incorporated into high-density polyethylene composites [114]. Here, the loss factor exhibits variations at high frequencies. The dielectric performance of microcrystalline cellulose in the ethylene vinyl acetate-vinyl ester of versatic acid terpolymer and $BaTiO_3$ has been reported to

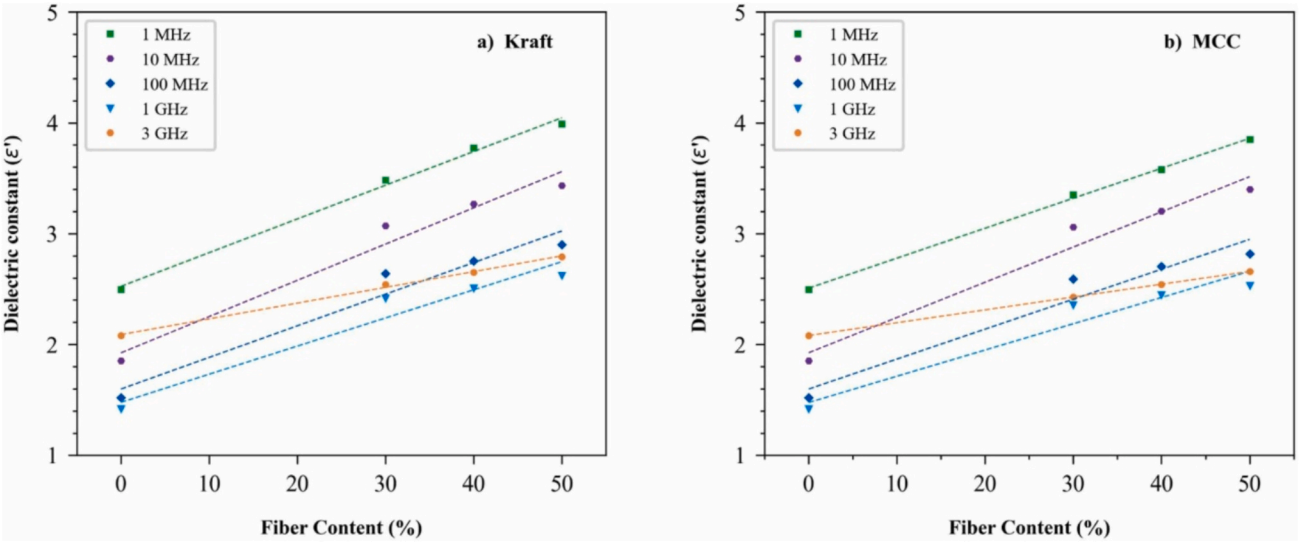

Fig. 10. The difference in the dielectric constant of (a) Kraft and (b) microcrystalline cellulose (MCC) composites with fiber content at different frequencies. Reproduced with permission from Elsevier 112.

have improved dielectric constant and reduced dielectric loss[115].

The general factors that influence the dielectric properties of polymer composites are frequency, temperature, chemical composition, humidity, and fabrication techniques. The increased cellulose fiber content generally leads to increased matrix–filler interface regions for cellulose fiber incorporated composites. Thereby, the polymer chains of the matrix can merely be displaced under the electric field. This displacement results in a space charge separation, which leads to an increased interfacial polarization and dielectric constant. The dielectric loss factor was also found to increase with cellulose fiber concentration, which specifies the retainment of electrical charges over a longer period. In addition to the fiber content, the hydroxyl groups and hydrophilicity of cellulose also play an important role in the dielectric performance. In the surface treatments to increase the hydrophobicity, water molecules are firmly bound to the surface hydroxyl groups of cellulose fibers, which always has a negative effect on the dielectric performance of cellulose composites [116].

Influence of structural design and fabrication techniques

Cellulose composites have been widely reported by incorporating carbon nanomaterials, metal or metal compounds, polymers, ceramics, and inorganic materials for various dielectric applications. Understanding and optimizing these structural parameters are essential for developing cellulose-based materials with desirable dielectric properties in the field of sensors, capacitors, and energy storage devices. The fabrication methods, processing techniques, and structural design of the matrix, as well as the distribution of the filler within it, influence the dielectric properties of cellulose composites. Orienting nanofibrillated cellulose in a specific direction significantly improves the dielectric permittivity in that direction [117]. The influence of dielectric properties on the effect of blending methods of cellulose with other materials has been reviewed by Xu *et al.* [104]. They investigated the dielectric performance of cellulose composites fabricated via physical blending and chemical blending. Here, we systematically review the fabrication strategies and processing routes of cellulose composites with different structural designs for dielectric and energy storage applications.

Films

Cellulose films typically comprise cellulose nanofibers or nanocrystals arranged in a matrix. The structural design of films, including the type and orientation of fillers, their alignment, and the packing density of cellulose nanomaterials, profoundly affects their dielectric

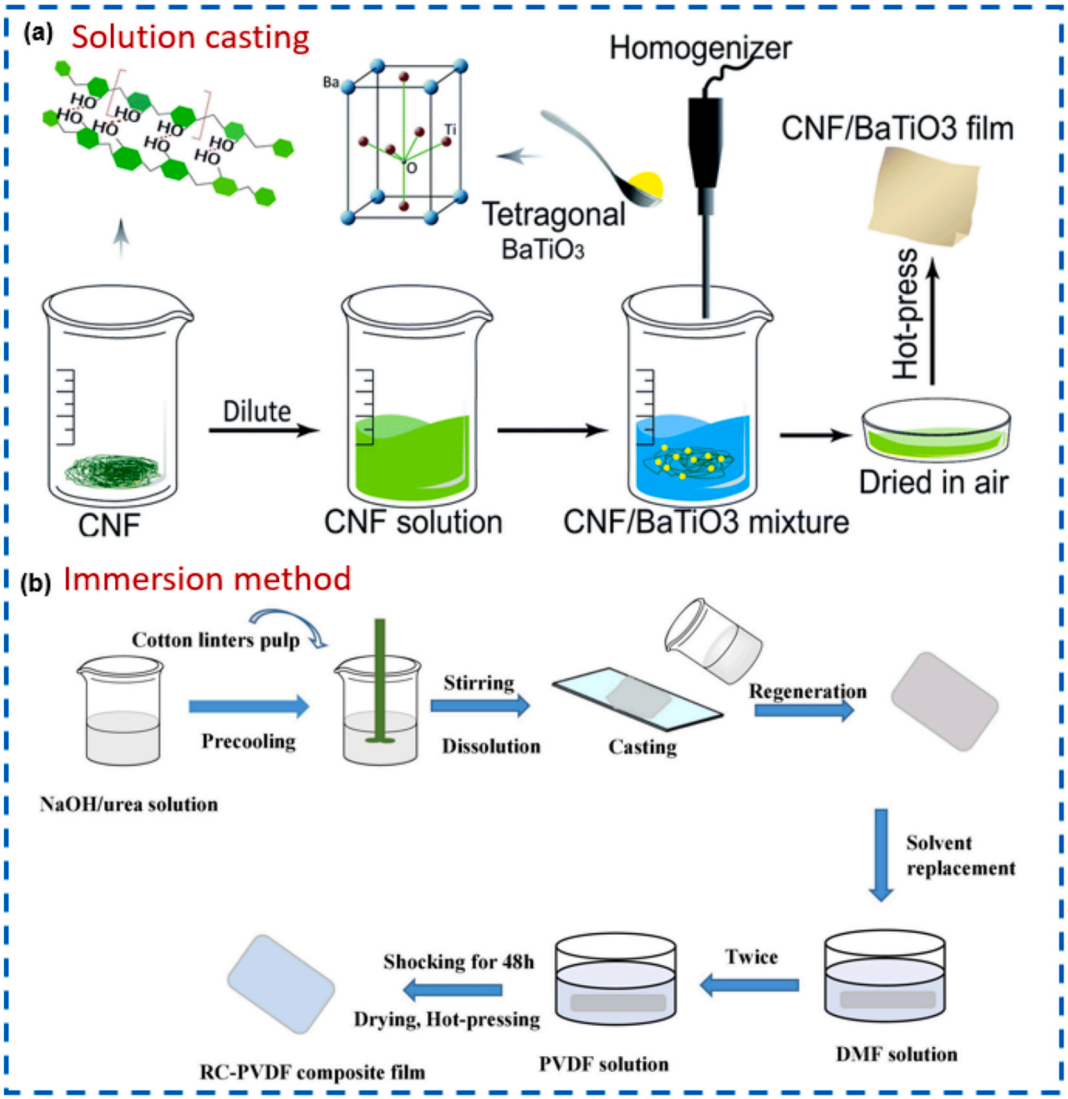

Fig. 11. Graphical illustration of the fabrication of (a) CNF/ $BaTiO_3$ nanocomposite films via solution casting. Reproduced from Ref. [9] with permission from the Royal Society of Chemistry. (b) RC-PVDF composite films via immersion method. Reproduced with permission from Elsevier [16].

properties and usage in large-scale equipment or portable devices. Dielectric films composed of pure cellulose-based composites exhibit a hydrophilic nature, which leads to insufficient polarization [118] and excessive dielectric loss after longstanding [119] and, thus, inferior energy storage performance. The alignment of cellulose nanocrystals within the film can influence the dielectric constant and anisotropy. Highly oriented structures can exhibit different dielectric responses along different axes. The film's interface between cellulose and other components (e.g., polymers or nanoparticles) affects polarization and charge storage, impacting the dielectric behavior.

Cellulose composite films can be fabricated in various ways for dielectric and energy storage properties, such as solution casting (as shown in Fig. 11a) [9,92,103], immersion method (as shown in Fig. 11b) [16], and vacuum filtration [120]. The composite film fabrication strategies mainly employ the mixing of cellulose and filler materials by physical methods such as stirring and blending (simple and environmentally friendly method but provides low compatibility) or via chemical attaching such as covalent bonding (complex process but provides good compatibility). Even though cellulose has abundant functional groups and strong compatibility with polar polymers, its compatibility with non-polar polymers and inorganic materials is not good and will impact its dielectric performance [121].

The dielectric parameters (ε' and ε'') and AC conductivity of the composite films of molybdenum trioxide (MoO_3) nanobelts incorporated with a blended mix of carboxymethyl cellulose (CMC)/poly(ethylene oxide) (PEO) are significantly improved with 8 wt% of MoO_3, for the applications in optoelectronic devices[92]. Wang *et* al. fabricated composite films composed of regenerated cellulose incorporated with 3 wt% PVDF by immersion method, exhibiting an energy storage density of 8.3 J/cm^3 under the electric field of 410 MV/m. These high-performing dielectric composites show 144 % and 176 % superior energy storage density than pure materials [16]. Deng *et* al. fabricated flexible composite films of CNF incorporated with $BaTiO_3$ by solution casting method without any organic solvents (Fig. 10a). The composite films exhibit an excellent dielectric constant of 188.03 for 30 wt% of $BaTiO_3$, approximately seven times greater than neat CNF. At the same time, the loss tangent has a slight rise from 0.70 to 1.21 at a frequency of 1 kHz [9]. The same group previously prepared TiO_2 incorporated CNF composite films and reported a dielectric constant of 19.51 and a dielectric loss of 0.51–0.81for 50 wt% of TiO_2 compared with pure CNF films at a frequency of 1 kHz [70]. Here, the incorporation of TiO_2 in the CNF matrix weakens the cellulose–cellulose attachment, which makes the film more porous and substantially impacts the dielectric properties. Generally, physical mixing strategies can cause lower breakdown strength and higher dielectric losses, which inhibits the longevity of composite films.

Surface treatments and chemical modifications are introduced to improve compatibility between cellulose and filler materials in composite films. Composite films composed of regenerated cellulose and $BaTiO_3$ nanofiber have been reported to improve the homogeneity and compatibility of matrix/fillers [79]. Here, $BaTiO_3$ nanofibers were surface modified by poly(dopamine), and the resultant composite film had greater breakdown strength and dielectric constant than pure films of RC and RC/$BaTiO_3$, as shown in Fig. 12. The dielectric films composed of dopamine-modified $BaTiO_3$ (2 vol%) showed 17.1 J/cm^3 discharged energy density at 520 MV/m, which is 40 % higher than unmodified film with similar composition at 460 MV/m. Here, the dopamine modification decreases the interfacial energy between $BaTiO_3$ nanofiber and

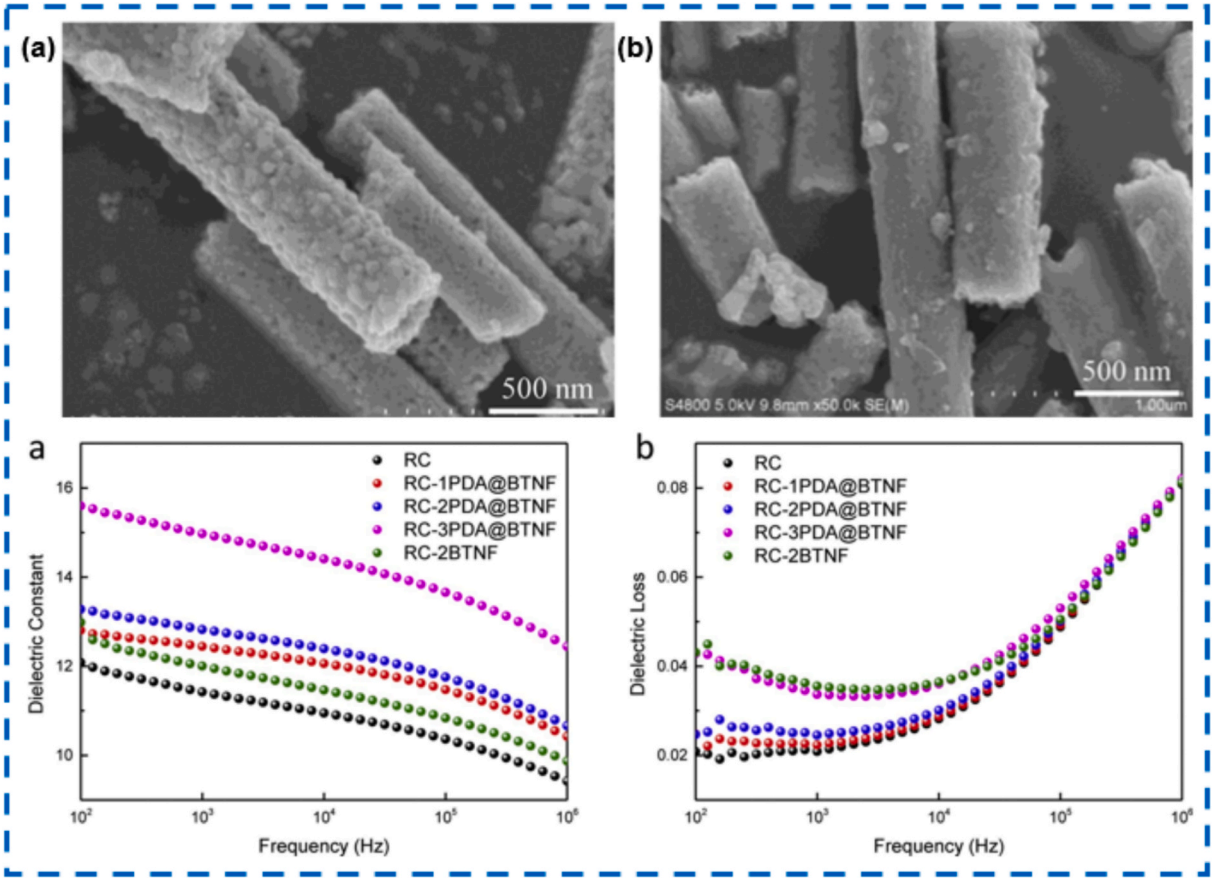

Fig. 12. SEM of (a) $BaTiO_3$ nanofibers and (b) poly(dopamine) modified $BaTiO_3$ nanofibers and frequency-dependent dielectric constant (a) and dielectric loss (b) for RC, RC-2 wt% $BaTiO_3$ nanofibers (RC-2BTNF) and RC-poly(dopamine) modified $BaTiO_3$ nanofibers composite films.
Reproduced with permission from Elsevier 79.

cellulose, preventing charge accumulation at the interface. Fly-ash (FA) coated polydopamine was incorporated into the RC matrix obtained from NaOH/urea aqueous solution fabricated by Shi *et* al. for improved dielectric properties [77]. At the 40 wt% of FA-coated dopamine in the RC matrix, the composite films showed an energy storage density of 2.57 J cm^{-3} and a breakdown strength of 260 MV $m^{-1,}$ about 8 times higher than neat RC films. Recently, Xu *et* al. reported a molecule-based modification strategy to improve the breakdown strength and dielectric constant of cellulose nanocrystals [120]. Here, alkali treatment and sulfonation improved the dielectric constant to 4.9 and 11.9, whereas TEMPO oxidation (2,2,6,6-tetramethylpiperidine-1-oxyl) and cyanoethylation further enhanced it as 11.1 and 13.2, respectively.

Aerogels

Cellulose-based aerogels offer low density, large specific surface area, high porosity, and good biocompatibility. It compensates for the shortcomings of brittleness and complexity of traditional silica aerogels. However, structural variations such as porosity, pore size, type of additives, and filler influence their dielectric and energy storage properties. The density and uniformity of the hydrogel network impact the effective permittivity and ion diffusion behavior, affecting dielectric constant and loss. Introducing nanoparticles into the hydrogel structure can modify its dielectric properties, enhancing energy storage or sensing functionalities. The interconnected porous structure of aerogels affects

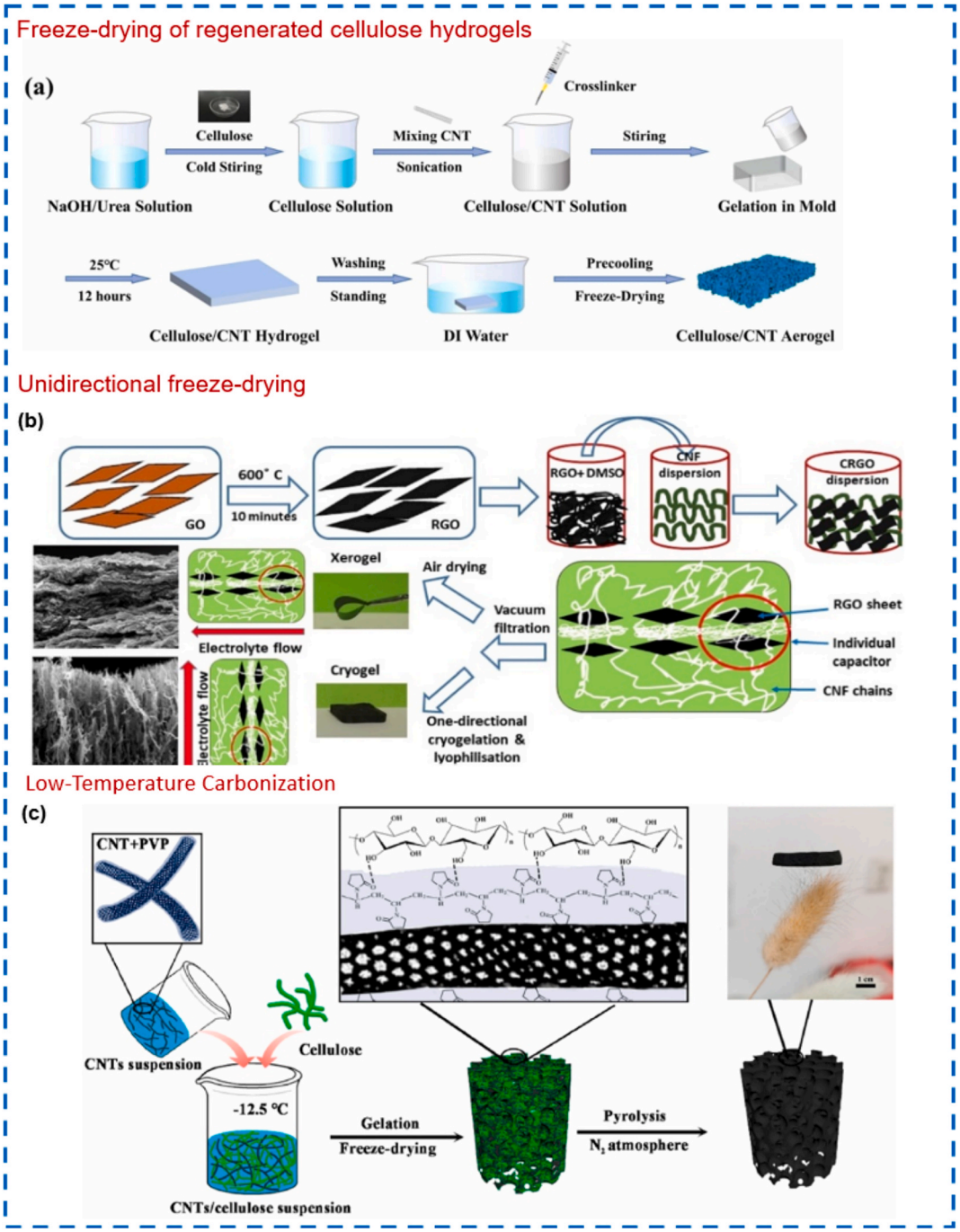

Fig. 13. Graphical illustration of the manufacturing process of (a) cellulose/CNT aerogel via freeze-drying of cellulose hydrogels. Reproduced with permission from Elsevier [122]. (b) cellulose nanofiber and reduced graphene oxide composite by air (xerogels) and unidirectional freeze (cryogels) drying. Reproduced with permission from Elsevier [54]. (c) carbon nanotube/cellulose aerogel via low-temperature carbonization. Reproduced with permission from Elsevier [124].

permittivity, as it determines the space available for charge accumulation and movement. Cellulose aerogels can be employed as electrodes, electrolytes, and separators for designing energy storage materials, such as supercapacitors since they possess high specific capacitance, excellent cycling stability, and improved energy and power density. Their 3D interconnected porous networks improve the robustness of mechanical properties and help the uniform distribution of filler materials, enabling the fabrication of stable electrode materials.

There are many ways to fabricate cellulose aerogels for dielectric and energy storage properties, such as freeze-drying [12254], in-situ polymerization and freeze-drying [123], low-temperature carbonization [124] freeze-drying and high-temperature pyrolysis[125] are the most used methods for fabricating cellulose-based aerogels. Cellulose/CNT aerogels have been fabricated as triboelectric nanogenerators by freeze-drying technique (as shown in Fig. 13a), which offers high specific surface area and improved dielectric performance [122]. Here, carbon nanotubes of uniform dispersion have been combined into the cellulose solution to enhance the conductivity and dielectric properties of aerogels. The effect of density, composition ratio, and porosity of composites incorporated with cellulose and reduced graphene oxide in the form of xerogels and aerogels were fabricated (as shown in Fig. 13b) by unidirectional freeze-drying to investigate their dielectric and electrochemical properties [54]. The resultant denser composite film shows a greater dielectric constant, ~85 (270 K) and ~164 (370 K), for a frequency of 1 MHz. In-situ polymerized cellulose/polypyrrole aerogel with freeze-drying was reported by Fu et al., which shows excellent elasticity, compressibility, and microwave absorption [123]. It is noted that for aerogels, the complex permittivity can be efficiently altered by changing the compression ratios. A low-temperature carbonization technique (as shown in Fig. 13c) has been employed to develop CNT/cellulose aerogel, which showed improved dielectric loss and thus improved microwave absorption performance [124]. A high-temperature pyrolysis method has been reported to fabricate composite aerogels with boron nitride and cellulose-derived carbon via freeze-drying technique [125]. The pyrolysis temperature and the boron nitride loading directly impact aerogel's dielectric loss capacity due to the ample interfaces and the polarization loss attributed to the pyrolysis-generated carbon defects.

Multilayered/ sandwich structured composites

A multilayered/sandwich film structure combines the benefits of polymers with dissimilar dielectric performances. The interfacial polarization between the end-to-end layers and the repressive growth of the electrical tree improves the dielectric constant and electric breakdown strength of such films[126]. Many researchers explored multilayered cellulose composites for improved dielectric and energy storage performance. Zhang *et* al. reported a strategy of hydrogen bond replacement to weaken the hydrogen bond network in cellulose and prepared sandwich-structured multilayered cellulose-based films using PVDF and $BaTiO_3$ nanoparticles[127]. The resultant multi-layered structure gives a superior energy storage density of 27.2 J cm^{-3}, which is much higher than the single-layered films. The attained outstanding energy storage performance arises from the high voltage endurance of cellulose and the interfacial polarization-coupled Schottky barrier height. The same group also reported multilayered film structures with cellulose/PVDF-$BaZr_{0.2}Ti_{0.8}O_3$ film and cellulose/PVDF-$Ba_{0.6}Sr_{0.4}TiO_3$ film via tape-casting technology and attained electrical breakdown strength (Eb) of 6.24 MV cm^{-1} energy storage density (ESD) of 31.07 J cm^{-3} and energy storage efficiency (η) of 80.03 % [128]. They demonstrated a theoretical basis for high-performing dielectric energy storage capacitors with low energy consumption and substituted cellulose instead of PVDF-based polymers for such applications. CEC and polyetherimide (PEI) based sandwich-structured dielectric films have been fabricated by Yan et al. and elaborated the breakdown mechanism of thin films [129]. The sandwich film achieved a high dielectric constant and an improved breakdown strength, and a high discharge energy density of 6.8 J/cm^3 at a temperature of 25 °C has been obtained. For positive sandwich-structured films (as shown in Fig. 14), PEI is used as an insulating outer layer to prevent charge injection from electrodes, and the CEC is used as a polarized intermediate layer, which can enhance the dielectric constant.

For multilayered/sandwich-structured composites, improvements in dielectric constants and breakdown strengths have been achieved because of the macroscopical interfacial polarization between the adjacent layers[130]. In the case of CEC and PEI-based multilayered films, a high value of dielectric constants was observed due to the high permittivity of CEC. Moreover, the macroscopical interfacial polarization formed by the accumulated charges between the CEC and PEI layers further improved the dielectric performance. As shown in Fig. 14, the layer interfaces are tightly connected without the presence of defects. Theoretically, the ε_r of a positively sandwiched film will increase with the increased content of the CEC layer. Similarly, for a negative sandwich film, the CEC is used as the outer layers (as shown in Fig. 14) and therefore the higher in content, thus high polarization and high tanδ. The finite element simulation models were explored to understand the breakdown mechanism of multilayered films, and a similar trend was observed.

It has already been reported that the suppressive growth of the electrical tree becomes wider at the interface and improves the ε_r and E_b of multilayer polymer films [126]. The electrical tree will be further extended due to the larger electric field gaps between layers so that the electrical trees cannot infuse the multilayered films [131]. In the case of CEC and PEI-based positive sandwiched films, the growth of the electrical tree is suppressed in the middle layer of the weak electric field due to the PEI layer's excellent insulating properties, resulting in the improved value of electric breakdown strength. As a summary, in the case of positively sandwiched films, the polarized intermediate layer and the insulating outer layer effectively prevent charge injection from electrodes, and thus, the polarized middle layer improves the ε_r of multilayer films. The interface between adjacent layers can act as a blocking region that traps the space charge and limits the growth of the electric tree because of electric field redistribution, which results in the improvement of E_b of multilayer films.

3D printed composites

The 3D printing technologies deliver the advantage of design flexibility and easy processability, which empowers the fabrication of dielectric materials in energy storage devices. Kim *et* al. previously reported that the 3D printing method offers homogeneous dispersion of ceramic nanoparticles and reduces the voids or cracks in the PVDF matrices, thus potentially improving the dielectric and energy storage performance of composites compared to conventional fabrication strategies.[132]. They achieved a higher dielectric property than solvent-cast PVDF films because of the presence of fewer defects, and the dipoles of polymer molecules are partly aligned during the 3D printing process. Recently, Wang *et* al. developed a 3D printing resin composites by grafting CNC into methacrylate malate photocurable resins (MMPR) to explore the advantages of design flexibility and high dielectric constant [133]. Here, the 3D-printed composites attained a dielectric constant enhancement from 4.0 to 10.9 at a frequency of 1 MHz. This would be due to the presence of abundant hydroxyl groups from the cellulose surface and the interface region between the cellulose-based fillers and the MMPR matrix, as shown in Fig. 15a. In addition to the dielectric performance, the breakdown strength and the energy density of composites show improvement compared to pure resin, which shows that the addition of cellulose plays an important role in enhancing energy storage performance. This work offers insights into developing 3D-printed photocurable resin composites for high dielectric constants applications. Lecoublet *et* al. studied the influence of the 3D printing technique, cellulose filler content, and size on the dielectric properties of

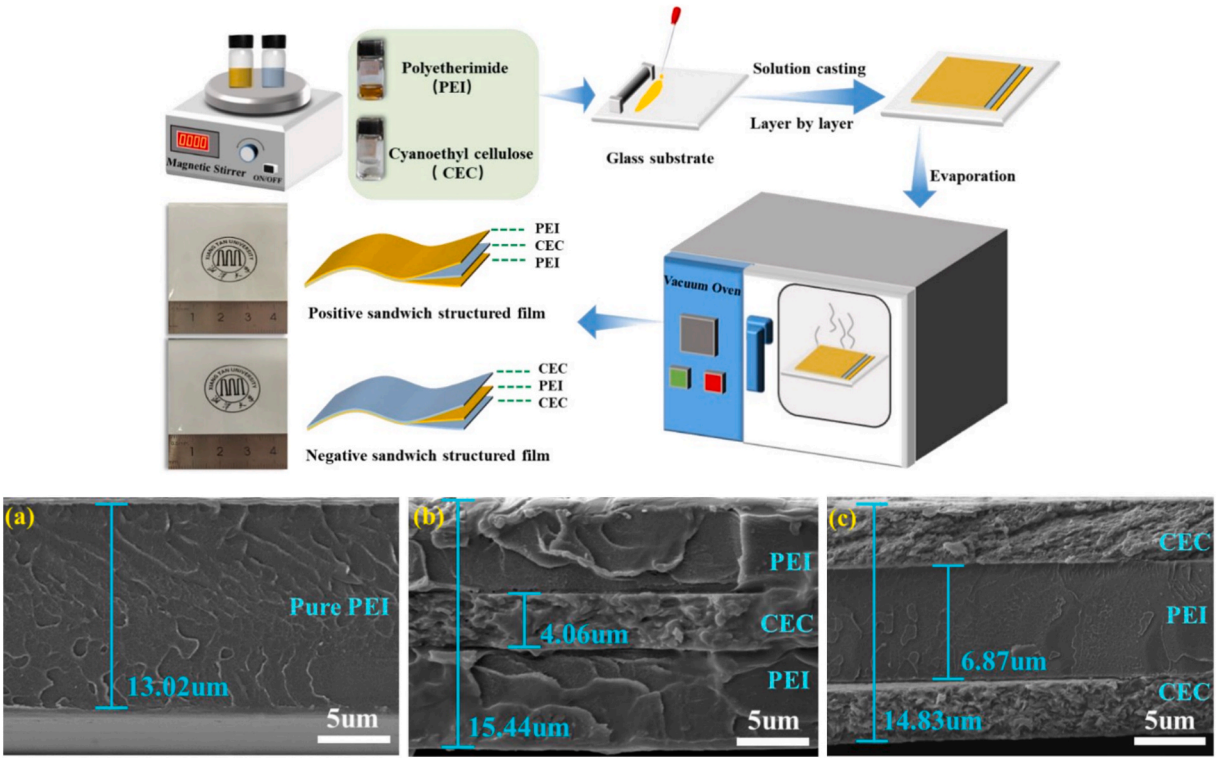

Fig. 14. Schematic of the fabrication process of sandwich-structured polyetherimide (PEI) and CEC dielectric films. The cross-section SEM images of (a) pure PEI film, (b) positive sandwich-structured film, and (c) negative sandwich-structured film for the sandwiched films.
Reproduced with permission from Elsevier 129.

composites comprising microcrystalline (MCC) and nanocrystalline (NCC) cellulose with polylactic acid (PLA) by fused filament fabrication [134]. The addition of cellulosic fillers increases the dielectric constant due to the higher crystallinity and polarity of cellulosic fillers. Interestingly, the 3D printed samples show reduced permittivity (Fig. 15b) compared to hot-pressed samples, which is attributed to the presence of printing defects such as voids or cracks through the 3D printing process [135].

Summary, Challenges, and outlook

This review comprehensively discusses cellulose composites, incorporating various filler materials, fabrication methods, structural designs, and their impact on dielectric and energy storage properties. The principles of dielectric and energy storage properties and how polymer composites can act as energy storage devices have been clearly described. Composites with cellulose as a matrix material and filler material are thoroughly reviewed, with different matrices and fillers, such as conductive fillers, ceramic fillers, metal oxide fillers, and hybrid filler-based systems. The fabrication strategies and structural design of such composites for dielectric performances also commence in the context of films and aerogels. Since electronic wastage is one of the biggest issues of humanity, the incorporation of cellulose-like biomaterials in dielectric and energy storage devices will be an excellent choice for the development of renewable dielectrics rather than synthetic polymers. Some of the conclusions from this mini-review are detailed here.

1. The general factors that influence the dielectric properties of cellulose composites are frequency, temperature, cellulose fiber content, humidity, and fabrication techniques.
2. Since different fabrication strategies have their own advantages in the dielectric and energy storage performance of cellulose composites, the parallel orientation of hydroxyl groups of cellulose to the film/aerogel surface is most important. Such orientation leads to stronger hydrogen bonding and excellent dielectric performance. For 3D printed composites, more research would be needed to optimize and improve the dielectric performance.
3. Besides parallel orientation, the hydroxyl groups and hydrophilicity of cellulose also play an important role in the dielectric performance. Hydrophobic film/aerogels provide good dielectric and energy storage performance because poor hydrophobicity leads to higher dielectric loss and even short circuits for long-term use.
4. The humidity and density of composites impact their dielectric and energy storage performance. Dielectric composites stored in humid atmospheres offer inferior performance, whereas a denser and more compact structure ensures a higher breakdown strength and results in high energy density.
5. For cellulose fiber incorporated composites, the increased cellulose fiber content generally leads to an increased matrix–filler interface regions, thereby leading to the displacement of polymer chains and, finally, an increased interfacial polarization and dielectric constant.

As shown in Fig. 1, substantial improvements have been made in the research of dielectric cellulose composites in the last few years, but many challenges still exist. Some of the challenges are detailed here.

1. The main challenge is the lack of commercialization, as the research is still restricted to the laboratory, and the fabrication processes are still dominated by conventional methods. This makes manufacturing more difficult for complicated structures and devices. Moreover, the durability and longevity of cellulose composites in energy storage and electronic devices require systematic research.
2. It is always challenging to accomplish a high dielectric constant whilst retaining a low dielectric loss in developing dielectric materials. For cellulose-based composites, this is even more challenging as strong hydrogen bonding tends to decrease dielectric permittivity.

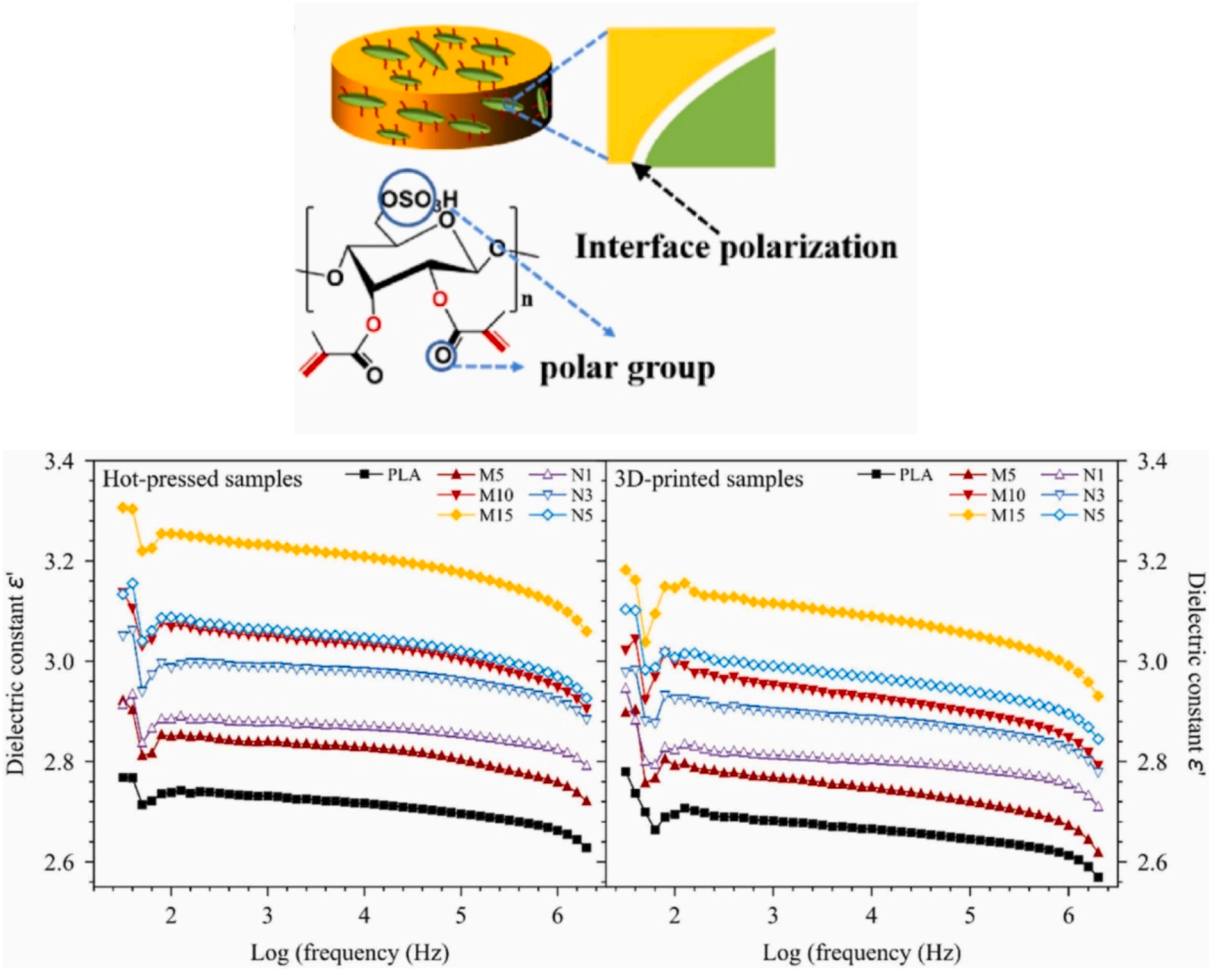

Fig. 15. Schematic representation of the polar groups and interface effects in composite materials. (a). Reproduced with permission from Elsevier [133]. Frequency-dependent dielectric constant of PLA-MCC-NCC composites prepared by hot-pressing and 3D printing. (b) Reproduced with permission from Elsevier [134].

3. Though the 3D network structure of aerogels benefits energy storage performance, their fabrication takes longer and consumes more energy, which limits mass production. Moreover, cellulose composite aerogels face practical difficulties in their dielectric testing, limiting their possible applications.
4. The cost and complexity of the chemical modifications of matrices and fillers for cellulose composite limit their dielectric performance.
5. The comparatively low mechanical properties of cellulose composites in commercial products are another barrier to their practical applications in electronic devices.

Nevertheless, there is significant progress in cellulose composites for dielectric and energy storage applications; there still remain a lot of areas to explore to comply with the current trend and future outlook for electronic devices. Some of the future outlooks are detailed here.

1. A more detailed and systematic approach must be established to develop the dielectric permittivity at a high-frequency band for microwave applications and to develop 5G communication functions.
2. Polar polymers, like cellulose, persisting in a high dipole density and substantial dipole moments, especially on crystalline structures, are capable of high-performance dielectric applications such as high-voltage capacitors, which are not much explored yet.
3. To further assess dielectric and energy storage performance in practice, the research should be combined with the latest simulation tools to simulate the performance of obtained cellulose composites.

CRediT authorship contribution statement

Mohammed Arif Poothanari: Writing – review & editing, Writing – original draft, Visualization, Validation, Software, Investigation, Formal analysis, Data curation. **Hanuma Reddy Tiyyagura:** Writing – original draft, Software, Methodology, Investigation, Formal analysis, Data curation, Conceptualization. **Yasir Beeran Pottathara:** Writing – review & editing, Writing – original draft, Visualization, Validation, Supervision, Software, Resources, Project administration, Methodology, Investigation, Funding acquisition, Formal analysis, Data curation, Conceptualization.

Declaration of competing interest

The authors declare that they have no known competing financial interests or personal relationships that could have appeared to influence the work reported in this paper.

Acknowledgments

The authors, Y.B.P. and H.T., would like to acknowledge the project DIGITOP, co-financed by the Republic of Slovenia, the Ministry of Higher Education, Science and Innovation, the Public Agency for Scientific Research and Innovation of the Research and Innovation of the Republic of Slovenia, and the European Union - NextGenerationEU.

References

[1] S. Tanpichai, A. Boonmahitthisud, N. Soykeabkaew, L. Ongthip, Carbohydr Polym 286 (2022) 119192, https://doi.org/10.1016/j.carbpol.2022.119192.
[2] A. Petritz, A. Wolfberger, A. Fian, M. Irimia-Vladu, A. Haase, H. Gold, T. Rothländer, T. Griesser, B. Stadlober, Appl Phys Lett 103 (15) (2013) 153303, https://doi.org/10.1063/1.4824701.
[3] A. Kafy, K.K. Sadasivuni, H.-C. Kim, A. Akther, J. Kim, Phys. Chem. Chem. Phys. 17 (8) (2015) 5923–5931, https://doi.org/10.1039/C4CP05921B.
[4] T. Nishino, N. Arimoto, Biomacromolecules 8 (9) (2007) 2712–2716, https://doi.org/10.1021/bm0703416.
[5] S. Tanpichai, S. Witayakran, J. Wootthikanokkhan, Y. Srimarut, W. Woraprayote, Y. Malila, Int J Biol Macromol 155 (2020) 1510–1519, https://doi.org/10.1016/j.ijbiomac.2019.11.128.
[6] B. Debnath, D. Haldar, M.K. Purkait, Carbohydr Polym 273 (2021) 118537, https://doi.org/10.1016/j.carbpol.2021.118537.
[7] R. Brooke,, K. Jain,, P. Isacsson,, A. Fall,, I. Engquist,, V. Beni,, L. Wågberg,, H. Granberg,, U. Hass,, J. Edberg, Annu Rev Mater Res 54(Volume 54, 2024) (2024) 1–25. doi: 10.1146/annurev-matsci-080921-084430.
[8] T.S.V.L.Z.H.C.K.J.K. S.H. Hassan Lee Hwei Voon, J Renew Mater 6(1) (2018) 1–25. 10.7569/JRM.2017.634173.
[9] J. Tao, S. Cao, R. Feng, Y. Deng, RSC Adv. 10 (10) (2020) 5758–5765, https://doi.org/10.1039/C9RA10916A.
[10] D. Ciuzas, E. Krugly, S. Sriubaite, I. Pauliukaityte, O. Baniukaitiene, M. Bulota, D. Martuzevicius, J Appl Polym Sci 139 (3) (2022) 51525, https://doi.org/10.1002/app.51525.
[11] A. Saini, D. Sharma, Y. Xia, A. Saini, X. You, Y. Su, L. Chen, C. Yadav, X. Li, Cellul. 28 (13) (2021) 8445–8457, https://doi.org/10.1007/s10570-021-04064-6.
[12] S.P. Raghunathan, S. Narayanan, A.C. Poulose, R. Joseph, Carbohydr Polym 157 (2017) 1024–1032, https://doi.org/10.1016/j.carbpol.2016.10.065.
[13] H. Tetik, K. Zhao, N. Shah, D. Lin, J Manuf Process 68 (2021) 445–453, https://doi.org/10.1016/j.jmapro.2021.05.051.
[14] J. Shi, L. Lu, W. Guo, J. Zhang, Y. Cao, Carbohydr Polym 98 (1) (2013) 282–289, https://doi.org/10.1016/j.carbpol.2013.05.082.
[15] L. Zhou, H. He, M.-C. Li, S. Huang, C. Mei, Q. Wu, Carbohydr Polym 189 (2018) 331–341, https://doi.org/10.1016/j.carbpol.2018.02.039.
[16] P. Wang, Y. Yin, L. Fang, J. He, Y. Wang, H. Cai, Q. Yang, Z. Shi, C. Xiong, Compos Part A Appl Sci Manuf 164 (2023) 107325, https://doi.org/10.1016/j.compositesa.2022.107325.
[17] S. Wang, C. Yang, X. Li, H. Jia, S. Liu, X. Liu, T. Minari, Q. Sun, J. Mater. Chem. C 10 (16) (2022) 6196–6221, https://doi.org/10.1039/D2TC00193D.
[18] E. Baer, L. Zhu, Macromolecules 50 (6) (2017) 2239–2256, https://doi.org/10.1021/acs.macromol.6b02669.
[19] D.K. Das-Gupta,, P.C.N. Scarpa, in: H. Singh Nalwa (Ed.), Handbook of Low and High Dielectric Constant Materials and Their Applications, Academic Press, Burlington, 1999,.
[20] Z. Ahmad, Polymer Dielectric Materials, IntechOpen (2012), https://doi.org/10.5772/50638.
[21] X. Wu, X. Chen, Q.M. Zhang, D.Q. Tan, Energy Storage Mater 44 (2022) 29–47, https://doi.org/10.1016/j.ensm.2021.10.010.
[22] M. A. Silaghi (Ed.), Dielectric Material, IntechOpen, 2012, 10.5772/2781.
[23] A.M. Badr, H.A. Elshaikh, I.M. Ashraf, J. Mod. Phys. 02 (01) (2011) 12–25, https://doi.org/10.4236/jmp.2011.21004.
[24] S.O. Nelson, S. Trabelsi, J. Microw. Power Electromagn. Energy. 46 (2) (2012) 93–107, https://doi.org/10.1080/08327823.2012.11689828.
[25] G.C. Psarras, Fundamentals of dielectric theories. In Dielectric polymer materials for high-density energy storage, William Andrew Publishing 11–57 (2018), https://doi.org/10.1016/B978-0-12-813215-9.00002-6.
[26] C. Komalan, M.A. Poothanari, H.J. Maria, S. Thomas, Polym Eng Sci 59 (11) (2019) 2195–2201, https://doi.org/10.1002/pen.25222.
[27] N. Ali, M. Bilal, A. Khan, R.K. Gupta, and Tuan Anh Nguyen, eds, Design, Synthesis, Functionalization, Properties, and Applications. Elsevier, Smart Polymer Nanocomposites, 2022.
[28] Nelson, Stuart O., and Samir Trabelsi. " Journal of Microwave Power and Electromagnetic Energy 46, 2 (2012), 93-107. 10.1080/08327823.2012.11689828.
[29] X. Yuan, J. Shi, Y. Kang, J. Dong, Z. Pei, X. Ji, Adv. Mater. 36 (3) (2024) 2308726, https://doi.org/10.1002/adma.202308726.
[30] F. Guan, J. Pan, J. Wang, Q. Wang, L. Zhu, Macromolecules 43 (1) (2010) 384–392, https://doi.org/10.1021/ma901921h.
[31] R. Gregorio, E.M. Ueno, J Mater Sci 34 (1999) 4489–4500, https://doi.org/10.1023/A:1004689205706.
[32] M. Samet, G. Boiteux, G. Seytre, A. Kallel, A. Serghei, Colloid Polym Sci 292 (2014) 1977–1988, https://doi.org/10.1007/s00396-014-3300-2.
[33] H. Sun, H. Zhang, S. Liu, N. Ning, L. Zhang, M. Tian, Y. Wang, Compos Sci Technol 154 (2018) 145–153, https://doi.org/10.1016/j.compscitech.2017.11.008.
[34] D.-H. Yoon, J. Zhang, B.I. Lee, Mater Res Bull 38 (5) (2003) 765–772, https://doi.org/10.1016/S0025-5408(03)00075-8.
[35] Q. Wang, L. Zhu, J Polym Sci B Polym Phys 49 (20) (2011) 1421–1429, https://doi.org/10.1002/polb.22337.
[36] Y. Rao, J. Qu, T. Marinis, C.P. Wong, IEEE Trans. Compon. Packag. Technol. 23 (4) (2000) 680–683, https://doi.org/10.1109/6144.888853.
[37] J. Mitali, S. Dhinakaran, A.A. Mohamad, Energy Storage Sav. 1 (3) (2022) 166–216, https://doi.org/10.1016/j.enss.2022.07.002.
[38] S.K. Ghosh, W. Rahman, T.R. Middya, S. Sen, D. Mandal, Nanotechnology 27 (21) (2016) 215401, https://doi.org/10.1088/0957-4484/27/21/215401.
[39] H. Xie, L. Wang, X. Gao, H. Luo, L. Liu, D. Zhang, ACS Omega 5 (50) (2020) 32660–32666, https://doi.org/10.1021/acsomega.0c05031.
[40] D. Wu, M. Luo, R. Yang, X. Hu, C. Lu, Materials 16 (2023) 12, https://doi.org/10.3390/ma16124201.
[41] Md.Z. Al Mahmud, J Nanomater 2023(1) (2023) 5432099. doi: 10.1155/2023/5432099.
[42] C.L. De Dicastillo, F. Rodríguez, A. Guarda, M.J. Galotto, Carbohydr Polym 136 (2016) 1052–1060, https://doi.org/10.1016/j.carbpol.2015.10.013.
[43] D.Q. Tan, Adv Funct Mater 30 (18) (2020) 1808567, https://doi.org/10.1002/adfm.201808567.
[44] Y. Yin, C. Zhang, W. Yu, G. Kang, Q. Yang, Z. Shi, C. Xiong, Energy Storage Mater 26 (2020) 105–111, https://doi.org/10.1016/j.ensm.2019.12.034.
[45] S. Zhang, J. Liu, Q. Guo, N. Wei, Y. Ning, Y. Bai, Y. Tian, T. Wang, Z. Sun, Y. Pu, Compos Part A Appl Sci Manuf 165 (2023) 107329, https://doi.org/10.1016/j.compositesa.2022.107329.
[46] S.M. Goodman, J. Che, W. Neri, J. Yuan, A.B. Dichiara, Energy Storage Mater 48 (2022) 497–506, https://doi.org/10.1016/j.ensm.2022.03.047.
[47] A. Kafy, A. Akther, M.I.R. Shishir, H.C. Kim, Y. Yun, J. Kim, Sens Actuators A Phys 247 (2016) 221–226, https://doi.org/10.1016/j.sna.2016.05.045.
[48] N. Madusanka, S.G. Shivareddy, P. Hiralal, M.D. Eddleston, Y. Choi, R.A. Oliver, G.A.J. Amaratunga, Nanotechnology 27 (19) (2016) 195402, https://doi.org/10.1088/0957-4484/27/19/195402.
[49] C. Jia, Z. Shao, H. Fan, J. Wang, RSC Adv. 5 (20) (2015) 15283–15291, https://doi.org/10.1039/C4RA13960G.
[50] S.P. Raghunathan, S. Narayanan, R. Joseph, RSC Adv. 6 (108) (2016) 107029–107039, https://doi.org/10.1039/C6RA21126G.
[51] K. Deshmukh, M.B. Ahamed, R.R. Deshmukh, S.K.K. Pasha, K.K. Sadasivuni, A. R. Polu, D. Ponnamma, M.-A.-A. AlMaadeed, K. Chidambaram, J. Mater. Sci. Mater. Electron. 28 (1) (2017) 973–986, https://doi.org/10.1007/s10854-016-5616-9.
[52] F. Wang, M. Wang, Z. Shao, Cellul. 25 (12) (2018) 7143–7152, https://doi.org/10.1007/s10570-018-2049-z.
[53] Y. Beeran P. T.,, V. Bobnar,, S. Gorgieva,, Y. Grohens,, M. Finšgar,, S. Thomas,, V. Kokol, RSC Adv. 6(54) (2016) 49138–49. 10.1039/C6RA06744A.
[54] Y.B. Pottathara, V. Bobnar, M. Finšgar, Y. Grohens, S. Thomas, V. Kokol, Polymer (guildf) 147 (2018) 260–270, https://doi.org/10.1016/j.polymer.2018.06.005.
[55] V.P. Anju, S.K. Narayanankutty, AIP Adv 6 (1) (2016) 015109, https://doi.org/10.1063/1.4940664.
[56] X. Zeng, L. Deng, Y. Yao, R. Sun, J. Xu, C.-P. Wong, J. Mater. Chem. C 4 (25) (2016) 6037–6044, https://doi.org/10.1039/C6TC01501H.
[57] V.P. Anju, S.K. Narayanankutty, Polymer (guildf) 119 (2017) 224–237, https://doi.org/10.1016/j.polymer.2017.05.034.
[58] Y.B. Pottathara, S. Thomas, N. Kalarikkal, T. Griesser, Y. Grohens, V. Bobnar, M. Finšgar, V. Kokol, R. Kargl, New J. Chem. 43 (2) (2019) 681–688, https://doi.org/10.1039/C8NJ03563F.
[59] M. Hasanin, A.M. Labeeb, Mater. Sci. Eng. B 263 (2021) 114797, https://doi.org/10.1016/j.mseb.2020.114797.
[60] X. Zheng, Y. Yin, P. Wang, C. Sun, Q. Yang, Z. Shi, C. Xiong, Int J Biol Macromol 243 (2023) 125220, https://doi.org/10.1016/j.ijbiomac.2023.125220.
[61] C. Zhang, Y. Yin, Q. Yang, Z. Shi, G.-H. Hu, C. Xiong, ACS Sustain Chem Eng 7 (12) (2019) 10641–10648, https://doi.org/10.1021/acssuschemeng.9b01302.
[62] Y.B. Pottathara, V. Bobnar, Y. Grohens, S. Thomas, R. Kargl, V. Kokol, Cellul. 28 (5) (2021) 3069–3080, https://doi.org/10.1007/s10570-021-03701-4.
[63] J. Tao, S. Cao, RSC Adv. 10 (18) (2020) 10799–10805, https://doi.org/10.1039/C9RA10915C.
[64] Z. Wang, J. Yuan, L. Zhao, J. Ren, Mater Lett 323 (2022) 132588, https://doi.org/10.1016/j.matlet.2022.132588.
[65] Q. Wang,, X. Liu,, Z. Qiang,, Z. Hu,, X. Cui,, H. Wei,, J. Hu,, Y. Xia,, S. Huang,, J. Zhang,, K. (Kelvin) Fu,, Y. Chen, Compos Sci Technol 227 (2022) 109601. doi: 10.1016/j.compscitech.2022.109601.
[66] M. Pusty, P.M. Shirage, RSC Adv. 10 (17) (2020) 10097–10112, https://doi.org/10.1039/C9RA10811D.
[67] S.-C. Shi, C. Chen, J.-L. Zhu, Y. Li, X. Meng, H.-D. Huang, Z.-M. Li, Appl Phys Lett 119 (2) (2021) 022903, https://doi.org/10.1063/5.0056164.
[68] K. Shi, H. Zou, B. Sun, P. Jiang, J. He, X. Huang, Adv Funct Mater 30 (4) (2020) 1904536, https://doi.org/10.1002/adfm.201904536.
[69] P. Sintharm, A. Nimpaiboon, Y.-C. Liao, M. Phisalaphong, Cellul. 29 (3) (2022) 1739–1758, https://doi.org/10.1007/s10570-021-04366-9.
[70] J. Tao,, S. an Cao,, W. Liu,, Y. Deng, Cellulose (2019). 10.1007/s10570-019-02495-w.
[71] Z. Zhang, S. Luo, S. Yu, Z. Guan, R. Sun, C.-P. Wong, Mater Des 142 (2018) 106–113, https://doi.org/10.1016/j.matdes.2018.01.009.
[72] C. Jia, Z. Shao, H. Fan, R. Feng, F. Wang, W. Wang, J. Wang, D. Zhang, Y. Lv, Compos Part A Appl Sci Manuf 86 (2016) 1–8, https://doi.org/10.1016/j.compositesa.2016.03.016.
[73] Y. Jiang, X. Xie, Y. Chen, Y. Liu, R. Yang, G. Sui, J. Mater. Chem. C 6 (32) (2018) 8679–8687, https://doi.org/10.1039/C8TC02900H.
[74] V.P. Anju, M. Manoj, P. Mohanan, S.K. Narayanankutty, Synth Met 247 (2019) 285–297, https://doi.org/10.1016/j.synthmet.2018.12.021.
[75] D.A. Gopakumar, A.R. Pai, Y.B. Pottathara, D. Pasquini, L. Carlos de Morais, M. Luke, N. Kalarikkal, Y. Grohens, S. Thomas, ACS Appl Mater Interfaces 10 (23) (2018) 20032–20043, https://doi.org/10.1021/acsami.8b04549.

[76] S. Sriphan, U. Pharino, T. Charoonsuk, P. Pulphol, P. Pakawanit, O. Khamman, W. Vittayakorn, N. Vittayakorn, T. Maluangnont, Nano Res 16 (2) (2023) 3168–3179, https://doi.org/10.1007/s12274-022-4957-3.
[77] J. Bao, J. Lao, Y. Hu, Y. Song, M. Xu, F. Niu, Q. Yang, C. Xiong, Z. Shi, Cellul. 30 (8) (2023) 5259–5271, https://doi.org/10.1007/s10570-023-05208-6.
[78] Q. Yang, C. Zhang, Z. Shi, J. Wang, C. Xiong, T. Saito, A. Isogai, ACS Appl Nano Mater 1 (9) (2018) 4972–4979, https://doi.org/10.1021/acsanm.8b01112.
[79] Y. Yin, C. Zhang, J. Chen, W. Yu, Z. Shi, C. Xiong, Q. Yang, Carbohydr Polym 249 (2020) 116883, https://doi.org/10.1016/j.carbpol.2020.116883.
[80] Y. Yin, J. He, C. Zhang, J. Chen, J. Wu, Z. Shi, C. Xiong, Q. Yang, Cellul. 28 (3) (2021) 1541–1553, https://doi.org/10.1007/s10570-020-03600-0.
[81] J. He, Y. Yin, M. Xu, P. Wang, Z. Yang, Q. Yang, Z. Shi, C. Xiong, ACS Appl Energy Mater 4 (8) (2021) 8150–8157, https://doi.org/10.1021/acsaem.1c01444.
[82] L. Wu, J. Zhao, Z. Li, Y. Zhai, Y. Zhang, Q. Zhen, Y. Cheng, X. Ding, P. Li, J. Liu, Z. Pan, J. Mater. Chem. C 10 (41) (2022) 15416–15423, https://doi.org/10.1039/D2TC02776C.
[83] J. Lao, H. Xie, Z. Shi, G. Li, B. Li, G.-H. Hu, Q. Yang, C. Xiong, ACS Sustain Chem Eng 6 (5) (2018) 7151–7158, https://doi.org/10.1021/acssuschemeng.8b01219.
[84] J. Yang, H. Xie, H. Chen, Z. Shi, T. Wu, Q. Yang, C. Xiong, J. Mater. Chem. A 6 (4) (2018) 1403–1411, https://doi.org/10.1039/C7TA08188J.
[85] M.L. Hassan, A.F. Ali, A.H. Salama, A.M. Abdel-Karim, J Phys Org Chem 32 (2) (2019) e3897.
[86] J. Li, J. Claude, L.E. Norena-Franco, S. Il Seok, Q. Wang, Chemistry of Materials 20(20) (2008) 6304–6306, https://doi.org/10.1021/cm8021648.
[87] M.N. Almadhoun, U.S. Bhansali, H.N. Alshareef, J Mater Chem 22 (22) (2012) 11196–11200, https://doi.org/10.1039/C2JM30542A.
[88] Y. Liu, B. Tang, Z. Wang, Y. Jiao, Q. Hou, Z. Dang, X. Hua, L. Wei, L. Wang, R. Wei, J Colloid Interface Sci 680 (2025) 85–95, https://doi.org/10.1016/j.jcis.2024.11.088.
[89] F. Gao, L. Zhou, K. Liu, Z. Feng, Q. Huo, C. Yang, T. Zhang, Y. Mao, D. Li, L. Wang, X. Hua, R. Wei, Chem. Eng. J. 493 (2024) 152830, https://doi.org/10.1016/j.cej.2024.152830.
[90] Z. Zhang, L. Zhou, L. Wang, Q. Hao, X. Hua, R. Wei, Nano Res 17 (8) (2024) 7574–7584, https://doi.org/10.1007/s12274-024-6678-2.
[91] G.R. Saad, Polym Int 34 (4) (1994) 411–415, https://doi.org/10.1002/pi.1994.210340410.
[92] A.A. Menazea, M.O. Farea, S.A. El-Khodary, Mater Chem Phys 312 (2024) 128585, https://doi.org/10.1016/j.matchemphys.2023.128585.
[93] Z.-M. Dang, J.-K. Yuan, J.-W. Zha, T. Zhou, S.-T. Li, G.-H. Hu, Prog Mater Sci 57 (4) (2012) 660–723, https://doi.org/10.1016/j.pmatsci.2011.08.001.
[94] İ. Mutlay, L.B. Tudoran, Fullerenes, Nanotubes and Carbon Nanostructures 22 (5) (2014) 413–433, https://doi.org/10.1080/1536383X.2012.684186.
[95] J. Tao,, S.A. Cao, DOI 10(1039) (2020) C9RA10915C.
[96] V.P. Anju, S.K. Narayanankutty, AIP Adv 6 (2016) 1, https://doi.org/10.1063/1.4940664.
[97] Y. Beeran, V. Bobnar, S. Gorgieva, Y. Grohens, M. Finšgar, S. Thomas, V. Kokol, RSC Adv 6 (54) (2016) 49138–49149, https://doi.org/10.1039/C6RA06744A.
[98] Y.B. Pottathara, S. Thomas, N. Kalarikkal, T. Grießer, Y. Grohens, V. Bobnar, M. Finšgar, V. Kokol, R. Kargl, New J. Chem. 43 (2) (2019) 681–688, https://doi.org/10.1039/C8NJ03563F.
[99] Y.B. Pottathara, V. Bobnar, Y. Grohens, S. Thomas, R. Kargl, V. Kokol, Cellul. 28 (2021) 3069–3080, https://doi.org/10.1007/s10570-021-03701-4.
[100] S. Dacrory, A.B. Abou Hammad, A.M. El Nahrawy, H. Abou-Yousef, S. Kamel, ECS J. Solid State Sci. Technol. 10 (8) (2021) 83004, https://doi.org/10.1149/2162-8777/ac1c56.
[101] F. Wang, M. Wang, Z. Shao, Cellul. 25 (2018) 7143–7152, https://doi.org/10.1007/s10570-018-2049-z.
[102] Z. Pan, L. Yao, J. Liu, X. Liu, F. Pi, J. Chen, B. Shen, J. Zhai, J Mater Chem C Mater 7 (2) (2019) 405–413, https://doi.org/10.1039/C8TC04555K.
[103] L.M. Al-Harbi, Q.A. Alsulami, M.O. Farea, A. Rajeh, J Mol Struct 1272 (2023) 134244, https://doi.org/10.1016/j.molstruc.2022.134244.
[104] Z. Wang, J.K. Nelson, J. Miao, R.J. Linhardt, L.S. Schadler, H. Hillborg, S. Zhao, IEEE Trans. Dielectr. Electr. Insul. 19 (3) (2012) 960–967, https://doi.org/10.1109/TDEI.2012.6215100.
[105] V.P. Anju, S.K. Narayanankutty, AIP Adv 6 (1) (2016) 015109, https://doi.org/10.1063/1.4940664.
[106] R. Tamura, E. Lim, T. Manaka, M. Iwamoto, J Appl Phys 100 (11) (2006) 114515, https://doi.org/10.1063/1.2372433.
[107] A. Ladhar, M. Arous, H. Kaddami, M. Raihane, M. Lahcini, A. Kallel, M.P.F. Graça, L.C. Costa, J Non Cryst Solids 378 (2013) 39–44, https://doi.org/10.1016/j.jnoncrysol.2013.06.018.
[108] A. Ladhar, M. Arous, H. Kaddami, M. Raihane, A. Kallel, M.P.F. Graça, L.C. Costa, J Mol Liq 196 (2014) 187–191, https://doi.org/10.1016/j.molliq.2014.03.040.
[109] A. Ladhar, M. Arous, H. Kaddami, Z. Ayadi, A. Kallel, IOP Conf Ser Mater Sci Eng 258 (1) (2017) 012001, https://doi.org/10.1088/1757-899X/258/1/012001.
[110] K. Chybczyńska,, E. Markiewicz,, A. Grząbka-Zasadzińska,, S. Borysiak, Ceram Int 45(7, Part B) (2019) 9468–76. doi: 10.1016/j.ceramint.2018.09.042.
[111] L. Xiang, J. Chen, Y. Yang, D. Xie, Y. Li, F. Liu, H. Ma, F. Wu, K. Chen, H. Wu, P. Lan, G. Yuan, S. Li, Q. Zhang, L. Gu, Y. Wang, J. Liu, J. Zhu, Polym Compos 40 (4) (2019) 1526–1535, https://doi.org/10.1002/pc.24892.
[112] A. Khouaja,, A. Koubaa,, H. Ben Daly, Ind Crops Prod 214 (2024) 118493. doi: 10.1016/j.indcrop.2024.118493.
[113] G. Das, S. Biswas, J. Reinf. Plast. Compos. 35 (8) (2016) 628–637, https://doi.org/10.1177/0731684415626594.
[114] A. Khouaja,, A. Koubaa,, H. Ben Daly, Ind Crops Prod 171 (2021) 113928. doi: 10.1016/j.indcrop.2021.113928.
[115] A. Zyane, F. Brouillette, A. Belfkira, R. Lucas, P. Marchet, J Appl Polym Sci 135 (15) (2018) 46147, https://doi.org/10.1002/app.46147.
[116] T.H. Mokhothu, M.J. John, Carbohydr Polym 131 (2015) 337–354, https://doi.org/10.1016/j.carbpol.2015.06.027.
[117] S. Xu, D. Liu, Q. Zhang, Q. Fu, Compos Sci Technol 156 (2018) 117–126, https://doi.org/10.1016/j.compscitech.2017.12.017.
[118] R. Tian, Q. Xu, C. Lu, X. Duan, R.-G. Xiong, Chem. Commun. 53 (56) (2017) 7933–7936, https://doi.org/10.1039/C7CC04240J.
[119] Y. Tu, B. Gong, C. Wang, K. Xu, Z. Xu, S. Wang, F. Zhang, R. Li, IEEE Trans. Dielectr. Electr. Insul. 22 (4) (2015) 2207–2213, https://doi.org/10.1109/TDEI.2015.004696.
[120] Q. Luo, Y. Liu, G. Zhou, X. Xu, Carbohydr Polym 324 (2024) 121451, https://doi.org/10.1016/j.carbpol.2023.121451.
[121] S. Cichosz, A. Masek, A. Rylski, Materials 13 (2020) 23, https://doi.org/10.3390/ma13235519.
[122] Z. Wang, C. Chen, L. Fang, B. Cao, X. Tu, R. Zhang, K. Dong, Y.-C. Lai, P. Wang, Nano Energy 107 (2023) 108151, https://doi.org/10.1016/j.nanoen.2022.108151.
[123] S. Feng, J. Deng, L. Yu, Y. Dong, Y. Zhu, Y. Fu, Cellul. 27 (17) (2020) 10213–10224, https://doi.org/10.1007/s10570-020-03497-9.
[124] Y.-Y. Wang, Z.-H. Zhou, J.-L. Zhu, W.-J. Sun, D.-X. Yan, K. Dai, Z.-M. Li, Compos B Eng 220 (2021) 108985, https://doi.org/10.1016/j.compositesb.2021.108985.
[125] D. Wang, M. Zhang, Y. Guo, T. Bai, H. Liu, C. Liu, C. Shen, J. Mater. Chem. C 10 (13) (2022) 5311–5320, https://doi.org/10.1039/D2TC00205A.
[126] X. Li, Z. Shi, M. Han, Q. Tang, P. Xie, R. Fan, Mater Today Energy 29 (2022) 101119, https://doi.org/10.1016/j.mtener.2022.101119.
[127] Z. Sun, J. Liu, H. Wei, Q. Guo, Y. Bai, S. Zhao, S. Wang, L. Li, Y. Zhang, Y. Tian, X. Zhang, H. Jing, Y. Pu, S. Zhang, J. Mater. Chem. A 11 (37) (2023) 20089–20101, https://doi.org/10.1039/D3TA04545E.
[128] Z. Sun, H. Wei, S. Zhao, Q. Guo, Y. Bai, S. Wang, P. Sun, K. Du, Y. Ning, Y. Tian, X. Zhang, H. Jing, Y. Pu, S. Zhang, J. Mater. Chem. A 12 (1) (2024) 128–143, https://doi.org/10.1039/D3TA05975H.
[129] C. Yan, H. Luo, X. Liu, Y. Liu, H. Luo, S. Chen, Mater. Today Sustainability 21 (2023) 100310, https://doi.org/10.1016/j.mtsust.2022.100310.
[130] X. Chen, J.-K. Tseng, I. Treufeld, M. Mackey, D.E. Schuele, R. Li, M. Fukuto, E. Baer, L. Zhu, J. Mater. Chem. C 5 (39) (2017) 10417–10426, https://doi.org/10.1039/C7TC03653A.
[131] L. Sun, Z. Shi, H. Wang, K. Zhang, D. Dastan, K. Sun, R. Fan, J. Mater. Chem. A 8 (11) (2020) 5750–5757, https://doi.org/10.1039/D0TA00903B.
[132] H. Kim, J. Johnson, L.A. Chavez, C.A. Garcia Rosales, T.-L.-B. Tseng, Y. Lin, Ceram Int 44(8) (2018) 9037–9044, https://doi.org/10.1016/j.ceramint.2018.02.107.
[133] Q. Wang,, X. Liu,, Z. Qiang,, Z. Hu,, X. Cui,, H. Wei,, J. Hu,, Y. Xia,, S. Huang,, J. Zhang,, K. (Kelvin) Fu,, Y. Chen, Compos Sci Technol 227 (2022) 109601. doi: 10.1016/j.compscitech.2022.109601.
[134] M. Lecoublet, M. Ragoubi, N. Leblanc, A. Koubaa, Ind Crops Prod 221 (2024) 119332, https://doi.org/10.1016/j.indcrop.2024.119332.
[135] M. Lay, N.L.N. Thajudin, Z.A.A. Hamid, A. Rusli, M.K. Abdullah, R.K. Shuib, Compos B Eng 176 (2019) 107341, https://doi.org/10.1016/j.compositesb.2019.107341.